5-2023

Use of Automatic Metaheuristic Optimizations for Boron Neutron Capture Therapy

Christopher Busch
University of Tennessee, Knoxville, cbusch1@vols.utk.edu

To the Graduate Council:

I am submitting herewith a thesis written by Christopher Busch entitled "Use of Automatic Metaheuristic Optimizations for Boron Neutron Capture Therapy." I have examined the final electronic copy of this thesis for form and content and recommend that it be accepted in partial fulfillment of the requirements for the degree of Master of Science, with a major in Nuclear Engineering.

Sandra Bogetic, Major Professor

We have read this thesis and recommend its acceptance:

Micheal Howard, Chester Ramsey

Accepted for the Council:
Dixie L. Thompson

Vice Provost and Dean of the Graduate School

(Original signatures are on file with official student records.)

Use of Automatic Metaheuristic Optimizations for Boron Neutron Capture Therapy

A Thesis Presented for the

Master of Science

Degree

The University of Tennessee, Knoxville

Christopher Busch

May 2023

I would like to dedicate this to family for supporting me throughout my life. Mom, Dad, Jack, and Emma Kate I hope I make you proud.

Acknowledgments

I would like to thank my PI Dr. Sandra Bogetic for her mentorship and advising these past 2 years, and the University of Tennessee dept. of Nuclear Engineering Graduate Research assistantship program for funding this project.

Abstract

Boron Neutron Capture therapy (BNCT) is a cancer treatment method investigated to reach malignant tumors that have added complications due to shape, size, or location. BNCT can deposit an immense dose gradient between the tumor cells and normal cells. This is done by selectively concentrating boron compounds in tumor cells and then irradiating all of the cells with an epithermal neutron beam. Due to the complex nature of neutron interactions, a high fidelity neutronic model is needed to design and predict the outcomes of a BNCT experiment. This work aims to introduce a high level autonomous optimization software, a metaheuristic code (GNOWEE) coupled with a high fidelity neutron transport code (MCNP6.2), to generically optimize a Beam Shaping Assembly (BSA) required for any BNCT scenario. This research work builds on previous work in the nuclear engineering field on metaheuristic optimization used to expand the optimization parameter space for a flexible BSA design. This thesis describes further efforts made in developing a generalized, problem independent Gnowee/MCNP6.2 software. The new software package includes the ability to design a BSA within a high fidelity model for possible future BNCT applications.

The expanded parameter space includes the exploration of different neutron sources (e.g. generator based or proton accelerator), of complex geometries, of optimization based on doses to the target, and cost constraints for possible BNCT treatment. Case studies were investigated and modeled for different tumor depth inside a patient's head setup, which resulted in a gradient of 10x the increase in tumor dose respectively to the healthy tissues. In addition, other models studied include the optimization of a BSA for a boron filled cell culture medium, which demonstrated the possibility to tailor any source to a primarily thermal neutron flux. This situation would demonstrate the first step toward a possible BNCT treatment. The results provide a powerful demonstration of the tailoring capabilities

of Gnowee/MCNP6.2 for BNCT application and provide improved capabilities to refine the spectrum of neutrons that are most effective for the treatment of both surface and deep-seated tumors.

Table of Contents

List of Tables

List of Figures

Chapter 1

Introduction

As human medical technology advances, human life expectancy increases [24]. The increase in life expectancy also leads to an increase in disease and burden on the global healthcare system, which will require for faster and more efficient treatments to accomplish a variety of different goals.

For example, Cancer requires a team with a diverse set of people and expertise to effectively treat the disease. Even some of the most common cancers can require complex treatments usually requiring multiple modalities such as surgery, chemotherapy and radiation therapy [31]. Some cancers are inoperable due to the tumor shape, size, or location, i.e. cancers such as Glioblastoma multiforme (GBM).

Currently, radiation cancer treatment is being performed using a wide array of technique's. While radiation therapy may have began with simpler external beam, the field has evolved to include adaptive therapy where changes in treatment delivery can occur while treatment is ongoing [5]. However cancer is still ever evolving and new therapy's and treatments must be investigated.

In addition, complicated and inoperable tumors can contribute to a reduction in effectiveness of conventional external beam radiotherapy. Conventional external beam therapy uses x-rays (photons) generated from electron interaction with a tungsten target to treat cancer[18]. An advantage of photon treatment is the ability for precise field shaping and energy tailoring. Another treatment is proton therapy which uses protons generated from a cyclotron for cancer treatment. Advantages of proton treatment include a relative

increase in RBE over photons, and the ability to have the photons stop in the tumor site leading to zero or drastically reduced exit dose when compared to photon treatment [18]. The main disadvantage concerning proton therapy is the increase in cost when comparing directly with photon therapy. This increase is estimated to be over double the cost which can make treatment access difficult [11].

An alternative radiotherapy, here investigated, is based on neutrons. What makes the neutron interesting is its ability to induce localized treatment reactions from stable isotopes. One of these proposed treatment methods that uses neutrons is Boron Neutron Capture Therapy (BNCT). BNCT is a treatment method developed to kill local tumors using short-range ions produced through the nuclear reactions between neutrons and ^{10}B isotope. The natural abundance of ^{10}B is about 20% of the total boron compound, and it has a very high thermal neutron absorption cross-section. Thermal neutrons are captured by ^{10}B, producing an alpha particles of 1.47 MeV and an a ^{7}Li ion of 0.84 MeV [15]. The generated alpha particles have a short range of 5–9 μm in tissue, delivering most of their energy to the tumor cells. This work examines the modeling of one such treatment method, Boron Neutron Capture Therapy (BNCT), for a complex inoperable cancer Glioblastoma multiforme (GBM).

While there have been BNCT in vitro studies in the past [13], the nature of the treatment is very challenging. From the initial patient selection, to being able to use neutrons at the required energies, advanced modeling work is needed for each BNCT.

The optimal energy of the neutrons depends on the type of neutron source, the patient size and the depth of the tumor. Thermal neutrons (<4eV) are suitable only for cancers which are located at near-tissue-surface because they are attenuated very rapidly in tissue. Epithermal neutrons (1 eV–10 keV) are essential for the treatment of deep-seated tumors. Epithermal neutrons are moderated in the healthy tissues, such as the patient head, losing their energy and become thermal neutrons at the cancer level. Nuclear reactors provide high-intensity neutron beams, however, they are located far from hospital and are not suitable for medical settings. Thus, the need to tailor neutron sources produced by generators (i.e., Deuterium-Deuterium or Deuterium-Tritium fusion generators) or proton accelerators (i.e., proton cyclotrons plus a stopping targets)[21]. However, so far no setup is known which fulfill

all of the IAEA requirements and based in a transportable neutron source. Thus, the need of adding to those sources a Beam shaping assembly (BSA) to tailor the neutron energies to the ones required to induce ^{10}B capture.

This work focuses on identifying an automatic, efficient framework, and method for producing several hypothetical treatment/experimental BNCT configurations from existing neutron sources. This is done by combining previous work on a neutron beam shaping assembly[28] and leveraging on advanced computational capabilities in the nuclear engineering field. The thesis outline the development of an increasingly flexible optimization methodology, that uses metaheuristic algorithm, to generate close to optimum BSAs configuration for various treatment scenarios. The tool used is a generic python based optimization, that can be used for difficult and conflicting nuclear engineering problems, GNOWEE [2, 3]. GNOWEE is here combined with a Monte Carlo based program, MCNP6.2 [30], for neutron transport prediction. MCNP6.2 performs dose calculations, neutron spectra identification, and allows for the various figure of merits to be evaluated quickly and efficiently. This thesis aims to demonstrate and provide a tool that can serve for providing the ideal neutron beam to accomplish all the IAEA recommendations for cancer treatments, using BNCT considering the advantages in time, safety, and cost of the treatment setup.

Section 1.1 introduces the scope and motivation for this work, as well as a discussion of the previous work upon which this thesis is based. Providing context and highlighting the impact of this thesis within the scope of BNCT and the need for a powerful, automatic, generic optimization algorithm. Moreover, Section 1.2 presents an overview of the structure of this thesis.

1.1 Motivation and Objective

Gliobastoma multiforme (GBM) and other types of inoperable cancers have some of the lowest survival rates of any disease in the world[14]. Patients who are often diagnosed with these diseases typically have no hope for curing the disease. The potential of a targeted treatment like BNCT could be life changing for this group of patients. In addition, targeted therapy's using neutrons could be expanded to other diseases and disease sites if BNCT is

initially proven to have some success. The difficulties of the BNCT treatment lay on 1) the ability to selectively delivery of boron to the tumor cells and 2) tailoring of the neutron spectra to induce ^{10}B capture, to increase the gradient of tumor dose over healthy tissues. This work focuses on defining a new advanced method for tailoring an ideal neutron beam to the tumor region, providing a new hope for BNCT.

The primary objective for this work is to propose new treatment potential for BNCT. This will be done by demonstrating the effectiveness of the GNOWEE/MCNP system for BNCT related purposes. In addition, this thesis focuses on demonstrating the viability of varying neutron sources for BNCT: Deuterium-Deuterium and Deuterium-Tritium neutron generator, Proton accelerators and possible new facilities, such as the UT fast neutron source, based on new generation reactors.

In addition to propose new treatment potential, this work also aims to demonstrate the possibility of a generalization of BSA for various BNCT configurations. As neutron sources cannot generate neutrons at every energy, an intermediate beam shaping assembly/energy tuner assembly (BSA or ETA) is needed for the possibility of BNCT. Previous work had been using a single BSA and a single neutron source to treat each individual disease site [28]. This would be very labor and cost intensive reducing the accessibility of BNCT. As a result this work will attempt to show a treatment of a differing disease site using a single source and BSA, and how effective treating differing tumor sites can be.

In addition, this work aims to the possibility to demonstrate the effectiveness of a generic metaheuristics algorithm could also alter the current state of optimizations. If a generic program can be used to bring together many different programs, experiences and capabilities, the functionality of said program would skyrocket. More users from various fields of study involved in the development, would bring newer updates and technologies. The potential of a widespread open source programming is not as common in current medical systems, mainly due to privacy risks, but if there is a space for it, further advancements in care and treatment would only further improve the overall system.

1.2 Thesis Outline

Chapter 2 presents the theoretical background of the BNCT methodology and the previous work done on BSA for inoperable tumors. Also introduces the modeling methodologies used for the optimization software, GNOWEE/MCNP 6.2. Chapter 3 describes the modeling technique used with GNOWEE/MCNP 6.2. The chapter provides an overview of the inputs, variables, constraints and objective functions used for the optimization of the BSA. As well, provides a brief overview of the enhancement done to previous version of the software to increase the generic capabilities. Chapter 4 introduces the results of the optimization and simulations of the BNCT configurations presented in Chapter 3. Finally, Chapter 5 summarizes the conclusions and lays out a plan for future work in Chapter 6.

Chapter 2

Background

The goal of this project is to enhance the methodology used for modeling neutron sources for Boron neutron capture therapy (BNCT) application.Previous work on beam shaping assemblies (BSA) is presented and discussed in Section 2.3. The cancer chosen for this work case study, the gliobastoma mutliforme (GBM), and its complications are discussed in 2.4. An overview of the optimization methodology chosen and further developed is introduced in Section 2.5. The optimization improvement on the BSA design is here presented by evaluating figures of merits on one of two targets, with also the introduction of the current inverse planning optimizations in medical physics.

2.1 Boron Neutron Capture Therapy (BNCT)

Boron Neutron Capture Therapy (BNCT) is a treatment where a neutron is captured by ^{10}B and a resultant ^{7}Li and α particle are released [20]. The advantage of this therapy is two fold. First, the ^{7}Li and α particles are high LET particles that lead to the exclusive killing of the cells containing the ^{10}B. Second, this therapy allows for the potential of highly selective therapy. If the neutron beam can be contained to a select area, the ^{10}B could absorb most of the neutrons while other neutrons will pass through the patient.

The first proposal of BNCT was by Locher in 1936 [17], followed by trials in the coming decades [16, 1, 27]. These trials were performed using reactors and the success of these

trials was mixed. The mixed success, and relative lack of improvement over conventional treatments lead to the end of BNCT trials in the United States.

After a brief hiatus, BNCT trials returned to the US and other western countries after trials in Japan demonstrated potential viability for melanoma [19], and grade 3 and 4 glioma [12]. The return of BNCT worldwide proved to be fleeting, as the only countries that have recently treated BNCT are Japan, Finland, and Taiwan. Again, these trials have been performed at reactor sites, which do have the advantage of a high thermal neutron flux, but a new future could for BNCT could lie ahead using neutron accelerator sources.

2.2 Neutron Production Methods

To make BNCT work, neutrons must be used. To date, most trials with BNCT have used a reactor based neutron spectrum [29]. A reactor spectrum has been used in the past due to the accessibility of the reactor, maximum neutron flux, and to minimize treatment time to reduce stress on patient [29]. This work will examine the use of established accelerator based neutron sources, and some new generation methods.

One of the accelerator options for neutron production is the Deuterium-Deuterium fusion generator (D-D). D-D generators generate neutrons of approximately 2.5 Mev [10]. The lower generated neutron energy when compared to other sources is an advantage for this accelerator. The reaction for the D-D generator involves 2 ^2H atoms colliding and forming a ^3He nucleus and a neutron [8]. An advantage of this neutron generator is that it can be operated as a steady beam or a pulsed neutron flux [8]. This could lead to a more precise neutron flux that could lead to more precise delivery of dose in the patient.

The Deuterium-Tritium fusion neutron generator (D-T) is another accelerator which has a reaction that uses a ^2H and ^3H fusion reaction that produces a ^4He and neutron [8].This accelerator produces neutrons at 14 Mev [7]. While the relative increase in energy, over other sources, makes scattering to the optimal therapeutic neutron energy more difficult, a main advantage of the D-T generator is the 2x increase in flux over the D-D accelerator [8].

An accelerator facility that is currently under construction that combines both a D-D and a D-T accelerator is the University of Tennessee Fast Neutron Source (FNS) [23]. This source

combines a D-D and D-T neutron source with natural Uranium [23]. This combination was developed to reduce cost and regulation for neutron source studies [23]. While this source may have a lower overall flux than the D-D and D-T accelerators by themselves [23], the primary thermal flux can be an advantage for some of the cell culture medium studies that will be discussed later. In addition to this work, the FNS has been combined with a similar GNOWEE/MCNP system to examine its feasibility for radioisotope production [25].

The final neutron production method that was examined was neutrons being produced through interactions by protons with a high Z target-proton neutron spallation (PNS) [21]. For this study, 4 PNS spectra were modeled in MCNP using two targets, Tungsten and Lead, and two beam energies, 100 Mev and 200 Mev protons. The reason for the two beam energies was due to a theoretical max (200 Mev) of a local cyclotron, and the limitation of cross section tables in MCNP6.2 (100 Mev) [30], above 100 Mev MCNP uses physics models which add computational time and increased uncertainty.

2.3 Beam Shaping Assembly

Due to the challenges presented by the existing neutron energy sources, a beam shaping assembly (BSA) or energy tuning assembly is needed to tailor the neutron spectra and that can be used to treat patients. This work aims to improve on past work. A reference work used here for comparison was performed at UC Berkeley in 2000 [28]. While the structure and components of the BSA largely appear the same, a set of stacked collimators or leaves were added to the end of the BSA for additional shielding and spectral shaping. Similar to the previous work, materials for the BSA were optimized, but in addition, the optimization process included the BSA dimensions as well. Figure 2.1 depicts the general structure of the BSA in relation to the "head" [28].

2.3.1 Field Shaping in Conventional Linear Accelerators

When considering field shaping for conventional linear accelerators there are two main components of the linear accelerators, Symmetric jaws and a multileaf collimator (MLC) [18]. Symmetric jaws work by making rectangular fields that can increase or decrease field size

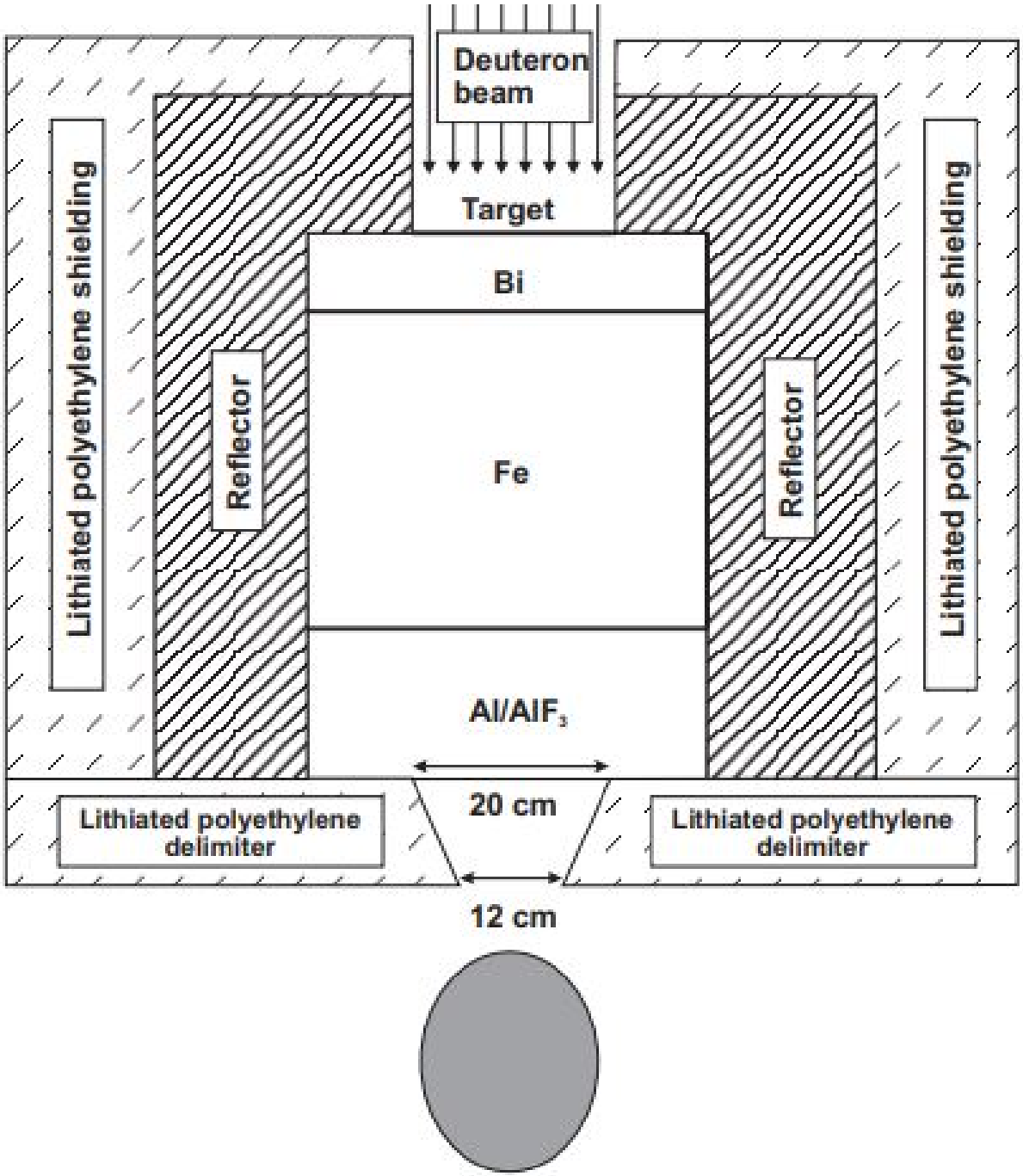

Figure 2.1: Depiction of the Beam Shaping Assembly used as reference for comparison[28]

depending on the disease site, objects at risk, or other treatment objectives. In addition to the jaws, MLC can account for additional field shaping. Unlike the symmetric jaws, the MLC is made of smaller individual "leaves" that can be expressed or depressed independently. The MLC allows for shaping that can appear irregular or asymmetric which leads to more precise dose delivery and coverage. The MLC can also rotate, which only adds to the precision of the delivery and treatment plans.

2.4 Case Study: Gliobastoma Multiforme

While Gliobastoma Multiforme (GBM) is the most common of gliomas [14] it is also the most aggressive. Current surgical, radiotherapy, and chemotherapy techniques have been unsuccessful in treating GBM due to the cancer's diffuse nature[14]. The diffuse nature causes difficulty in imaging, as the central tumor mass is apparent, but the individual cells or tendrils might not be visible. This can lead to the spread of GBM to vital part of the brain which will eventually lead to death[14]. While there have been challenges in human treatments, there have been promising results in the realm of animal studies [13]. Immunotherapies have shown that animals are resistant to the implementation of GBM like tumors; however, the aggressiveness in animals is difficult to replicate, and more work needs to be done in this area[14, 13]. Gliobastoma multiforme is a complex and deadly disease that needs novel therapies to advance survival rate and potentially cure this disease.

2.5 Optimization Methodology

While the use of an optimization method for a topic such as BNCT is novel, in the wide field of medical physics, optimizations with treatment objectives are relatively common place.

2.5.1 Optimization in Medical Application

A typical optimization method used in medical treatments is called inverse planning [18]. In short, inverse planning is the process of optimizing to a set of end goal objectives, by changing the patient set up. For inverse planning optimization algorithms, there are two

groups of variables the input parameters that are being optimized, and the desired end goal objectives. End goal objectives include, but are not limited to, desired dose to the gross tumor volume and any object at risk dose constraints. This part of the optimization can also be called clinical objectives. Input parameters are also called beam parameters and can include leaf gap, edge length, and complexity score [9]. Inverse planning optimization has become more common as the treatment modalities it was designed become the standard in radiotherapy. The treatment modalities that use inverse planning most commonly are intensity modulated radiotherapy (IMRT) [9] volumetric modulated radiotherapy (VMAT) [6], 3D conformal [22], and tomotherapy [26].

2.5.2 Optimization of a Beam Shaping Assembly and leaves for BNCT

Designing BSAs and stacked collimators for different neutron sources, and tumors shapes and depths, is a complex optimization problem that includes multiple variable, objective functions and constraints. The chosen optimization method combines a metaheuristic algorithim and a monte carlo program to investigate potential outcomes for a BNCT treatments. The metaheuristic algorithm software chosen and in this work enhanced is GNOWEE. The neutron transport code used to model the source, the BSA and the patient with the tumor is MCNP6.2. The upcoming subsections will explain the various components, variables, and constraints chosen for this BNCT optimization.

GNOWEE- A General Purpose Hybrid Metaheuristic Optimization Algorithm

The metaheuristic algorithm used, GNOWEE, is a modular, Python-based, open-source, hybrid optimization algorithm, designed for rapid convergence to nearly globally optimum solutions for complex, constrained engineering problems. The basic tenets of GNOWEE are the building of a function that takes in a feature vector and outputs of a single fitness value. The foundation of the program allows the user to use GNOWEE for a variety of different programs and models[3].

The feature vector is a user-defined list of variable values for GNOWEE to chose from. These options are variables that can be of continuous, discreet, integer, or combinatorial nature. GNOWEE rapidly samples potential combinations of variables and relies on the user-defined objectives to assess the various candidates' performance. The user defined objective is defined in a separate function which evaluates the model output to determine a single number, the fitness, for GNOWEE to use in its evaluation and evolution towards the optimum result.

MCNP- Monte Carlo N-Particle Transport Code System

MCNP [30] is a general-purpose, time-dependent Monte Carlo transport code which uses continuous-energy and generalized geometry. It has been implemented in the nuclear field for the verification of a wide variety of radiation transport problems, especially those related to neutron simulations. The default cross section data used by MCNP consists of the ENDF/B-VII libraries [30]. Due to its inherent simplicity and high regards, it was the most viable option for an optimization framework that required python code to automatically manipulate respective variables. The main limitations of the coupled GNOWEE/MCNP6.2 codes are on the MCNP side, due to long computational time required for each model. The easiest way to reduce this computational time was to reduce the number of particles or introduce variance reduction techniques; however, this also could have potentially increased uncertainty in each model. As a result, there was an error propagation added into the post processing evaluation of each file.

Chapter 3

Methodology

The below section will give an overview to the modeling work performed for the BNCT. This work combines a metaheuristic algorithm with a monte carlo program to consider a range of sometimes conflicting objectives to achieve the most optimum model. In this Chapter the newly developed framework that couples the two codes and provides the objective functions, the fitness calculations, the running script on the University of Tennessee cluster and MCNP outputs evaluation for the BNCT application, is outlined. For each of the optimized case studies the chapters introduces the variables, sources, constraints and objective functions.

3.1 Development of the GNOWEE/MCNP Framework for BNCT

For this study, a framework was developed to couple GNOWEE to a Monte Carlo neutron transport code (MCNP 6.2 [30]).This was done to evaluate a beam shaping assembly (BSA) in regards to certain dose objectives and constraints. Each of the MCNP inputs that were created were run for a set number of particles, and a fitness value was calculated for each input. After the initial population generation, these fitness values were then compared to the best population of previous fitness values. If the current fitness was better than a current parent, the parent was replaced, and this optimization continued either until convergence,

the model stalled out (no steady improvement), or a set maximum evaluation number was reached.

Figure 3.1 shows the GNOWEE/MCNP coupled process.

While the main functions of the original GNOWEE remained unchanged, a few enhancements were added that allowed for the speed of GNOWEE to increase by up to 70 times in some cases. The modification that made for the largest improvement to the run time of GNOWEE was the 'batch submit' feature to improve parallel running of the multiple evaluations. This improvement allowed for GNOWEE to submit models to be run on any available cores which improved from the earlier series submission, where each file was run one after another.

In addition to this speed-up, a redundant evaluation eliminator (aka "weeded children" function) was added. Weeded children on average demonstrated a triple time speed-up. Weeded children eliminated the generation and re-submission of runs that have already been evaluated. Without this add-on, these old feature vectors were still evaluated alongside the new feature vectors. While in some instances concerning Monte Carlo evaluation, it could be advantageous to run the same model multiple times, for GNOWEE this was not so. This was because GNOWEE would not average out all the fitness from each evaluation, and instead would only take the most current calculated fitness value[4].

3.2 Optimized Case Studies for BNCT

For this study, 5 case studies are being considered to ensure the strengths and the validity of the optimization methodology used for BNCT. In the 5 case studies, different neutron sources (i.e.,neutron generators versus proton induced neutron) and targets (head versus cell colture) are being introduced and results provided. Each of the case studies are described in this section, in terms of neutron source and target type, variables, constraints and fitness functions.

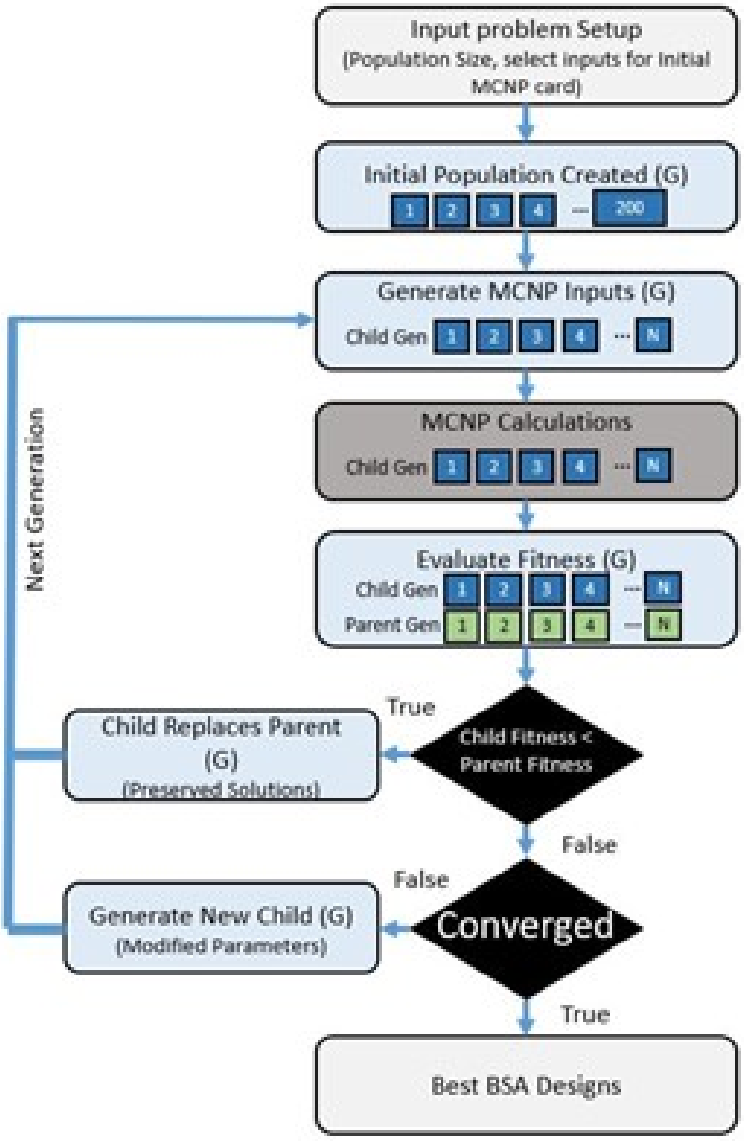

Figure 3.1: Beam-shaping assembly optimization process. (G) indicates processes performed by GNOWEE.

3.2.1 Geometric Design and User Defined Variables

The BSA included as initial geometry 3 layers of cylinders, with the inner most layer comprised of 3 different cylinders of various sizes. When discussing the design and user defined variables for the optimization the starting point was with the variable that picked the neutron source. The source was the starting point as it informed the rest of the BSA design. Depending on the constraints for the the chosen optimization (Hammond, Malcolm, Sattler, Grant, and Spielberg) the optimization could have chosen from accelerator sources (D-D, D-T, or the FNS), or any of the PNS sources (proton origin energy: 100 or 200 Mev, target: W or Pb). After the source variable was chosen, there were 2 categories of variables that informed the geometric design of the BSA: the variables concerned with the BSA size, and variables concerned with the BSA materials.

The first set of user defined variables were the BSA size variables. There were 6 of these variables. There were two variables that chose the overall design for the BSA. The first variable chose the BSA height. This variable ranged in 10 cm increments from 150.1 to 80.1 cm. The inferior boundary of the BSA was located at 10.1 cm. The second variable chose the BSA radius multiplier. While there are other variables that chose the actual dimension of the BSA radius, this variable chose if those radii would be multiplied by 1, 0.75, 0.50, or 0.25. This variable was chosen to allow for the BSA to change in size depending on the target. The other 4 variables chose the exact radii of the outer neutron shield (65, 67, 69, 71, 73, 75, 77, 79), the outer reflector radius (35, 37, 39, 41, 43, 45), the inner scattering cylinders (12, 13, 14, 15, 16, 17), and the exit bore for the BSA (7, 8, 9, 10, 11). The previous 4 variables were listed in units of cm and could be multiplied by the radii multiplier variable giving maximum flexibility for the BSA design.

The next set of variables was the materials of each of the BSA components. There were 7 BSA components that could have material optimization. These components were the outer shield, the reflector, the 3 inner scattering blocks, and 2 final foils located directly superior to the BSA exit bore. The exact materials were run dependent and were chosen from the expansive or reduced material list. These lists can be found in tables 1 and 2 the Appendix. Figure 3.2 depicts the overall model optimization.

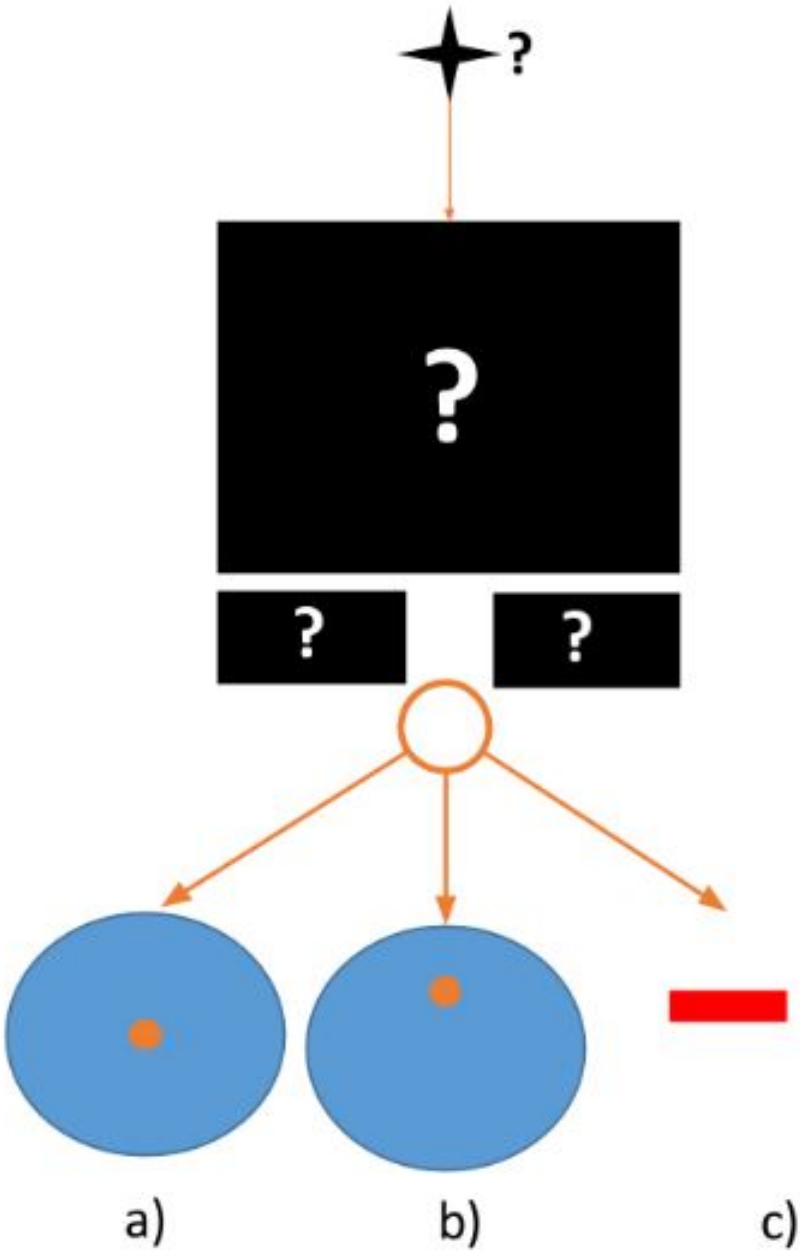

Figure 3.2: Basic structure of model optimization. Black areas indicates what is being optimized. Three targets are going to be studied: a) head with a tumor in the center, b) head with a tumor shifted towards the surface, and c) a tumor cell culture. Targets a) and b) are located directly inferior to the stacked collimator opening, and target c) is located 4 cm inferior to the stacked collimator opening.

After the BSA variables were optimized, there were additional variables that optimized the stacked collimator. The first variable that could be optimized was the selection of the number of collimators: 5, 7, or 9. Depending on that selection, there was a minimum of 20 dimensional variables and 5 material variables, or a maximum of 36 dimensional variables and 9 material variables. The dimensional variables allowed the algorithm to chose the boundaries in the x and y planes. This could be done irregularly meaning, that the boundaries within the x and y planes did not have to be symmetrical, and as a result this decision allowed for maximum model flexibility. The boundaries ranged on one side from -15, -12, -9, -6, -3, -1 cm on the negative axis and 1, 3, 6, 9, 12, 15 cm on the positive axis. Like the BSA material lists, the material list for the collimators had to match and can be found in tables 1 and 2 in the Appendix.

The final set of variables were target variables. These variables were separated based on whether the target was the head setup or the cell culture medium setup. The only variable that could have been optimized was the tumor tissue. The difference between the variables was the concentration of Boron. The concentration could be chosen to be 30μg , 40μg , or 50μg. Due to uncertainty surrounding the diffusion of Boron in a hypothetical patient, the surrounding tissue contained 10 μg of Boron, meaning that there was the ability for the algorithm to chose from a $3x$, $4x$, or $5x$ increase in concentration on the targeted tissue.

3.2.2 Constraints

With every model there were constraints and decisions made for each of the variables, and outcomes of each simulation. The initial part of this discussion will center on the variable constraints, and then there will be a discussion about the constraints placed on the simulation outcome.

The first constraint was on each variable to be in discrete lists instead of continuous or integer lists. This decision was made to give increased flexibility while keeping the realistic manufacturing parameters in case the optimum BSA were to be built. In some early instances of this project the algorithm would chose continuous variables with precision less than 0.00001 and that was not realistic if a BSA were to be built when considering machining precision. Another constraint was a treatment time of 1 hour. This was decided as if there was ever to

be a treatment, patients could become uncomfortable if a treatment exceeded this length. The next constraint was on the maximum size of the BSA. This constraint was the BSA could not be larger than the initial BSA model it was based on [28]. This decision was made as if the new hypothetical BSA were to exceed this size it could be very difficult to set up, and could lead to inconsistencies or damage to the BSA. The materials were separated out again due to experimental realism. The reduced material list (2) was chosen in case there was an option to perform a future experiment. Cost and ease of acquiring materials was the driving factor of this constraint. A constraint on the collimators not being able to fully close was put in place so there could always be some sort of unobstructed neutron beam leaving the BSA. If there was an obstruction, there could be no way of ensuring a neutron beam that could be used for treatment was going to interact with the target. There was a constraint placed on location of the target in both the head and cell culture medium set ups. This was done to eliminate the potential for file writing errors, and to provide maximum neutron interaction. The final constraint concerning the setup was with the target Boron concentration. The Boron concentration in the targeted tissue was constrained to 3-5x the surrounding tissue due to uncertainty over absorption and concerns about possible Boron poisoning. Without performing experiments with a compound there was no way to know exact absorption numbers, and the limit on Boron in the patient without harmful side effects.

In addition to the model setup constraints there were up to 3 constraints on the model outcome. The first constraint was on all models and that was that every file had to run to completion. In some instances, there could have been error in file writing leading to lost particles, but the tallies could have been calculated up to that point. If this error occurred it could pollute the model results and therefore the 1 million particle constraint was added to eliminate this scenario. The next two constraints were only for the head setup models with neutron accelerator sources (Hammond and Spielberg). These constraints were a maximum and minimum calculated tumor dose. The maximum dose was 60 Sv and minimum was 0.2 Sv. The maximum dose constraint was decided based on clinical objectives for treatment plans using a gamma knife system, and the lower constraint was to keep the algorithm from choosing too low of doses. These constraints were eliminated for the Sattler run as the estimated neutron flux was too low to produce a dose of that minimum without violating

the previous 1 hour treatment time constraint. Finally, if any of the components of the fitness calculation such as tumor dose, ideal neutron spectra, neutrons exiting the BSA, or ideal reaction are calculated to be zero this will violate a constraint. This was implemented to prevent an optimum from being reached due to an undefined or unwanted zero component of the objective function evaluation.

3.2.3 Objective Function

Four different GNOWEE/MCNP6.2 runs were completed. Every run had a population size of 15 and a maximum evaluation number of 10,000. The runs were grouped by neutron source type. The source types included neutron generator-based reactions from D-D or D-T generators, or spallation neutrons, produced from proton interaction with a high Z material such as Tungsten or lead. The run comparison was split up as the difference in neutron flux was 3-4 orders of magnitude in some cases. Another difference in the runs was the target. Each source type had a run with a model of a head, and a separate run with a cell culture setup.The input fitness for each of the models will be between 0 and 1, with the ideal being at 0. The head run used an intensive fitness formula shown below in Equation 3.1, and the the cell culture run used the fitness formula shown in Equation 3.2.

$$f(x) = [X_d \cdot X_n \cdot X_\phi] + 3 \cdot \delta \tag{3.1}$$

$$f(x) = 1 - (X_\alpha / X_\sigma) \tag{3.2}$$

Figures of merit for the first function, equation 3.1, that were considered included X_d equivalent dose ratios of tissue and tumor dose and skin and tumor dose, X_ϕ the incident neutron spectra, X_n the total neutrons that can be used for treatment, and δ the total model uncertainty.. Equation 3.2 considered figures of merit that were the reaction types (X_α and X_σ).

The material list also varied depending on target. This was due to the possibility of practical experimentation. A reduced material list, table 2, was paired with the cell culture target, and an expansive list, table 1 was paired with the head model. All runs had the option

to swap out every material, change the size of the assembly, its respective components, and the option to choose the stacked collimator setup (5, 7, or 9 stacked collimator "leaves" before the target).

After the neutron generator base run with the expansive material list was completed, a fifth run began. This run also used a head model; however, the tumor location was moved 5 cm closer to the source. Due to this change in setup, a new fitness formula was used. For this scenario, the "optimum" spectra component was removed. This equation is shown below in 3.3. For this run, the Hammond optimum dimensions and materials were used, with the exception of the leaf setup. The number of leaves could be 5, 7, or 9, with any material shown in the table 1, and with any dimension for those leaves. This model only considered the dose ratios, X_d, the total neutrons that can be used for treatment X_n, and the total uncertainty δ.

$$f(x) = [X_d \cdot X_n] + 3 \cdot \delta \tag{3.3}$$

3.2.4 Preparation and Initialization

The optimization began by inputting each list into the GNOWEE run file. There was a parent population of 15 set, a maximum number of generations set to 10,000. The initial 15 parent population was found following 150 evaluations using the LHC sampling method. Since it was impossible to reach a global convergence of 0 without violating a previous constraint, the run will terminate when two consecutive parent population are identical [2].

3.3 Challenges

The main challenge for these models was the run time of MCNP6.2. This problem was alleviated on the GNOWEE end by implementing the batch submit ability. The batch submit feature allowed for the use of all available cores on a computing system. As only one file can run on one core this way to improve run time could only be improved by improving the overall computing system through adding more or newer cores. Another way this problem was addressed was by reducing the number of particles run per model. Again, the reduction

of particle number would increase uncertainty, but an uncertainty component was added to the fitness evaluation to account for this problem. Another challenge presented was the limitation to one fitness value being optimized. If there was the ability for each component to be evaluated independently, there could be an improvement for the overall model. In the future it might be advantageous to investigate this problem as a multi-objective problem with each component evaluated as its own fitness component.

3.4 Solution Evaluation

An added functionality to the GNOWEE/MCNP coupling was the ability to view the parents vector at any time in the run. As neutrons are stochastic, and there was increased uncertainty due to the reduction in particles run, the option to investigate a variety of optimal models was informative. As a result, the optimum model from each set was chosen and evaluated individually to investigate each figure of merit for the maximum amount of information.

Chapter 4

BSA Optimization

In this Chapter, the idea is to design an optimized BSA to sufficiently modify the identified sources neutron spectra to satisfy BNCT objective functions. All five optimum BSA's will be identified and described for the 5 case studies.

4.1 Optimization Results

A primary goal of this project was to demonstrate the ability for GNOWEE/MCNP to evaluate a diverse set of solutions rapidly to allow for the widest possibility for potential treatment. The GNOWEE/MCNP models evaluated 32,355 potential solutions across all four BSA optimizing runs. The GNOWEE/MCNP models took 29 days of real time to run to completion between the four set ups. Due to the setup of the computing system and the GNOWEE/MCNP program, all of the runs, with the exception of the Spielberg, were run simultaneously. As a result, each evaluation period occurred over a two week period. During the full run, each of the files took approximately 6 minutes to run. If these files were ran serially, the total model run would have taken between 3 and 6x as long to run (up to 174 days of total run time). This work would not have been feasible without the improvement in the structure and submission of the GNOWEE/MCNP framework. In addition, the effective file run time for the GNOWEE/MCNP run was 1.37 minutes. This was calculated by performing a weighted average of the 4 runs that were run simultaneously. A key part of GNOWEE/MCNP's advantage has been its ability, to have rapid convergence.

This was demonstrated by the dramatic decrease in evaluation time. Running a full source/BSA/head with tumor simulation is computationally expensive and time-intensive, especially when improved statistics are needed at the level of the tumor and skin dose. Furthermore being able to evaluate thousands of simulations simultaneously thanks to the GNOWEE/MCNP framework is remarkable and would help accelerate the pace of the BSA for BNCT deployment. Table 3 in the Appendix contains the evaluations, and time for each of the runs.

When comparing the simulated models from the different case stud the different run setups must be considered. For this section, the two runs using the head model and full materials library, the Hammond and Sattler runs, will be compared. Comparisons were also done using the Malcolm and Grant models as those models used the cell culture medium and reduced material library set up.

As shown in Table 4 in the Appendix, there is a significant difference in the calculated doses for the Hammond and Sattler models (tumor dose 20.03 Sv for Hammond vs 3.62E-5 Sv for Sattler). The decrease in tumor dose in the Sattler case study can primarily be attributed to the decrease in neutron flux from the neutron spallation target, when compared to neutron sources. Further work should be done for the PNS set up to measure the total integrated neutron flux that can be achieved from this setup. Results in this thesis are based on MCNP6.2 simulation. All that withstanding, the dose ratios for the Sattler run were an observable improvement over its counterpart the Hammond run. This improvement in the Sattler run demonstrated that a higher equivalent dose was calculated at the tumor site, than in the Hammond run. While this was a modest increase, with a ratio of tissue dose to tumor dose being 0.09 for the Hammond run and 0.13 for the Sattler run, there was a calculated increase which could mean that if the PNS flux can be comparable to the accelerator flux the PNS setup could be more advantageous in the future. Both the Hammond and the Sattler runs were comparable in terms of the percentage of neutrons that exited the BSA (35.2% vs 34.9%). Again, if the PNS can be scaled up in terms of neutron flux, this neutron production method could be an improvement over current methods. Proton neutron sources can change and be scaled in intensity for different cyclotrons types, the reference used for this research was on what is available in the Knoxville proton therapy health Center (reference?). The

calculated uncertainty for the models were also comparable at 0.16 for the Hammond and 0.12 for the Sattler run. A final note is that it would be difficult to see the effects of dose in a patient using the Sattler setup due to the estimated dose being so low, meaning that with current technologies, it would be more advantageous to use the Hammond set up if possible.

The cell culture medium runs, Malcolm and Grant, were more similar than the Hammond and Sattler runs. This was primarily due to the constraints put in place. The goal of these optimizations were to model a potential experimental setup, so there was a reduced material library used for the optimization. In response to this constraing, both of these models consisted primarily of polyethylene. An advantage or polyethylene is due to the neutron scattering properties of hydrogen, which is the main element of the material. This would allow for the most amount of scattering and absorption of the unwanted or non ideal neutrons. In terms of the fitness, the Malcolm model showed an improvement over the Grant run (3% optimal reaction vs 0.9%). The increase in the reaction rate for the Malcom BSA is attributed to the decrease in initial energy of the neutrons (14 Mev vs 100 Mev). The birth energy of the neutrons is higher for the PNS due to the reaction and the initial energy of the protons. In the future if there is a cyclotron that can produce protons at a high enough flux, but lower energy this could be advantageous, but with current technologies there are limits on the ability for this method of neutron production. The similrity of this two case scenario, ensure the importance of using the proton spallation source at the Proton Center, Knoxville as proof-of-concept facility for cell culture experiment.

4.2 Top Performing Candidates for each case study

The below results are divide into 2 subsections based upon the type of neutron sources for the case studies (neutron vs proton neutron spallation). The case study are then split in two based upon the material library used. An additional section is based around the ability for a generalization of the BSA for BNCT. This additional section is an "improvement" on one of the previous BSA optimums

4.2.1 BSA for BNCT using Neutron Generator Sources

Best BSA Candidate for the Expansive Material Case Study : Hammond

The Hammond run was an intensive run that used the extensive list of materials see table 1 located in the Appendix, and the head model and the equation 3.1 fitness, and neutron accelerator sources.

The optimum design given by the GNOWEE/MCNP Hammond run had a GNOWEE/MCNP fitness of 0.367. The chosen source for this BSA was the D-T generator. The total BSA length was 70 cm. The BSA featured an outer neutron shield, inner neutron reflector, 3 internal scattering blocks, and 2 final scattering foils. The BSA radii, and and materials can be found in the Appendix in tables 5 and 6.

The optimum design had 5 collimators, with the collimators opening centered on the center of the Head. Part of the head was shielded by other collimators which was expected as the goal is to minimize dose to the healthy tissue. The leaf materials can be found in table 7 in the Appendix. Figure 4.1 depicts the ideal BSA for the Hammond run.

When compared to other GNOWEE/MCNP BSA designs, the materials for the Hammond model were less homogeneous. There was no polyethylene materials chosen. This BSA designed was designed using a variety of pure metals and compounds compared to the commonly seen plastics. The lack of material homogeneity is likely due to the increase in available for the optimization to use, which allowed the optimizer to chose materials that may be more optimum for neutron scattering, but are more difficult to procure. In addition, the radius of this particular BSA was on the larger side. This is due to the larger relative target of the head, and therefore to improve the neutron coverage wider scattering blocks and cylinders were needed to construct this BSA

Best BSA Candidate for the Limited Material Case Study: Malcolm

The Malcolm run used the reduced list of materials see table 2 located in the Appendix, the cell culture medium target model, the equation 3.2 fitness, and neutron accelerator sources. This model was run with the intent of it being performed experimentally in a university setting.

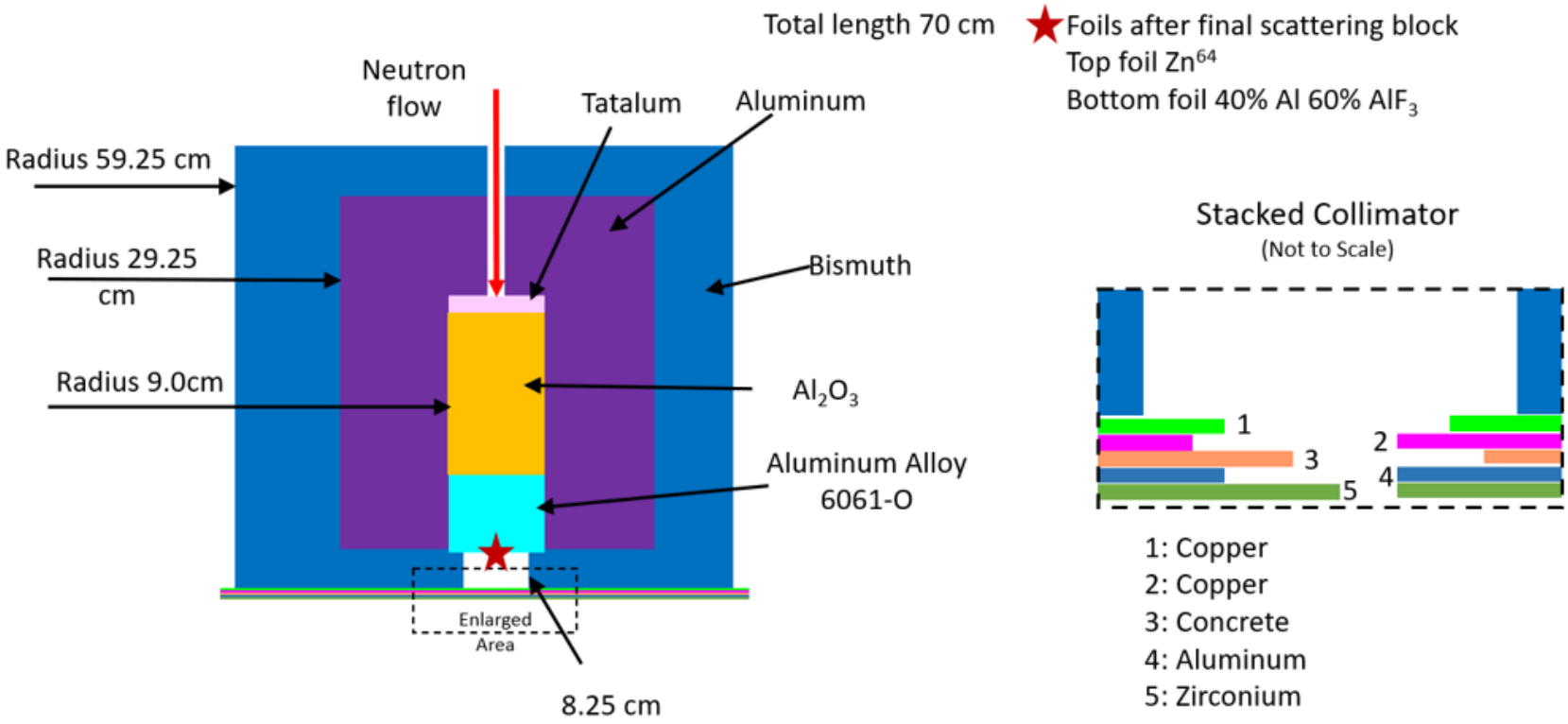

Figure 4.1: Visual depiction of Hammond BSA Design

The optimum design given by the GNOWEE/MCNP Malcolm run had a fitness of 0.970601, meaning that approximately 3% of all reactions were the ideal optimized reaction. Similar to the Hammond BSA, the chosen source was the D-T generator, and the total Malcolm BSA length was also 70 cm. The Malcolm BSA components were the same as the Hammond, and the BSA radii, and and materials can be found below in tables 8 and 9. Figure 4.2 depicts the ideal BSA for the Malcolm run.

The optimum design had 9 collimators, with the collimators opening centered on the center of the cell culture medium. This is expected, as the neutrons should spread out to cover the cell culture medium surface. The increase in collimators is likely due to the desire to have an increase in the thermal flux of neutrons due to the lack of depth of the cells on the cell culture medium, and the elimination of the "optimal spectra" figure of merit. The leaf materials can be found in table 10.

The main parts of the Malcolm BSA consisted of varieties of polyethylene, with the exception of the top scattering foil (lead) and the middle scattering block (Iron). The material homogeneity was expected due to the properties of hydrogen when considering neutron shielding. In addition the optimization chose the maximum number of collimators. This decision was made as the increased number of collimators increased the thermal neutron flux which in turn increased the reaction rate in the cell culture medium. In addition, the Malcolm BSA radius was on the smaller end, and that was due to the smaller target of the cell culture medium.

4.2.2 BSA for BNCT using Proton Neutron Spallation Sources

Best BSA Candidate for the expansive Material case study: Sattler

The Sattler run was an intensive run that used the extensive list of materials found in table 1 located in the Appendix, the head model, the equation 3.1 fitness, and the PNS neutron source.

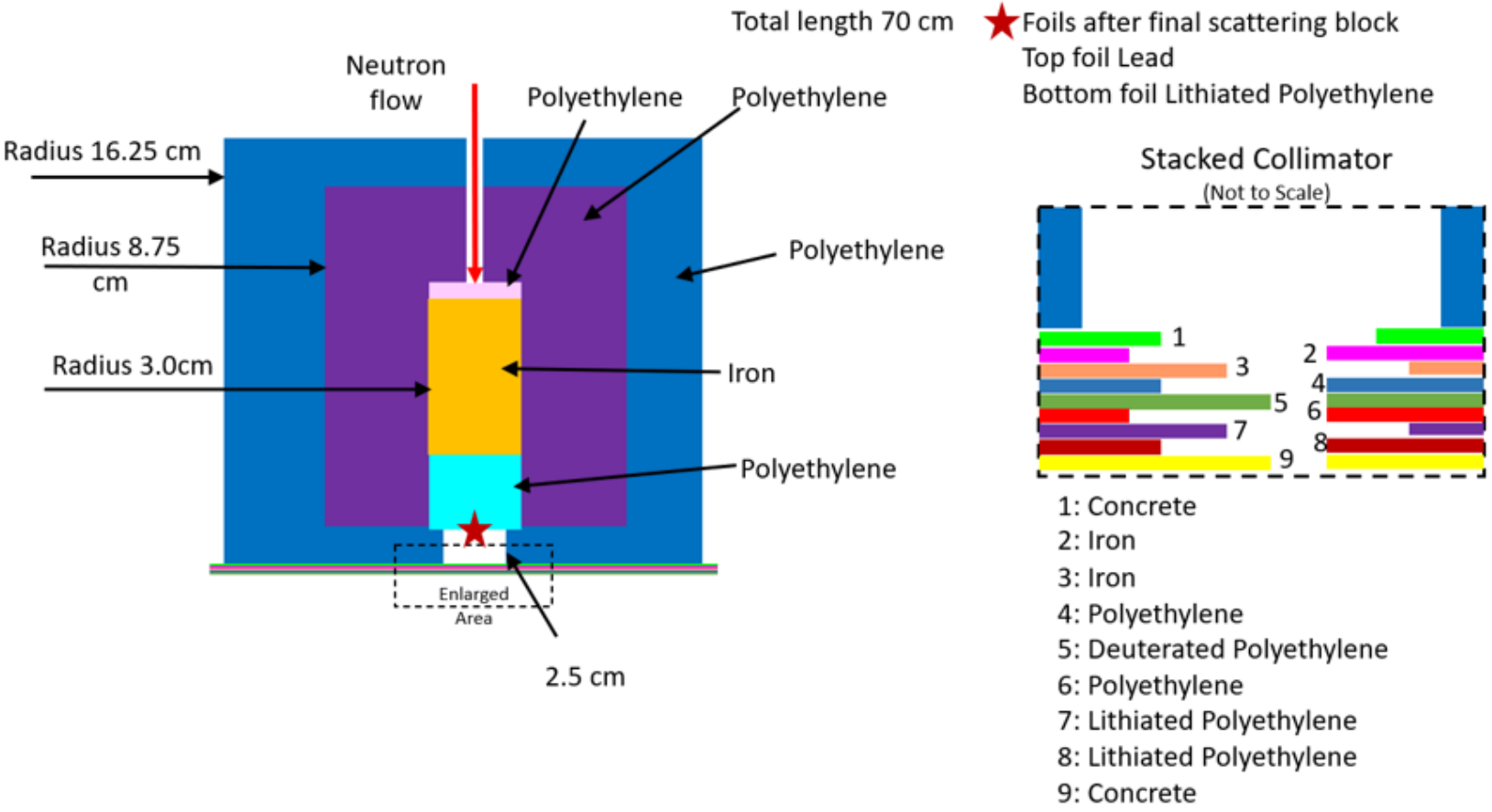

Figure 4.2: Visual depiction of Malcolm BSA Design

The optimum design given by the GNOWEE/MCNP Sattler run had a fitness of 0.397. The chosen source was the 200 Mev proton beam with a tungsten target. Similar to other runs, the overall BSA length was 70 cm, and the individual BSA component structure remained the same. The Sattler BSA radii, and and materials can be found in the Appendix in tables 11 and 12. Figure 4.3 depicts the ideal BSA for the Malcolm run.

Like the previous head setup run, the optimum design consisted of 5 collimators, with the collimators opening centered on the center of the head model. Also like the Hammond run before, the collimators shielded parts of the head that did not contain the tumor in order to decrease dose. The leaf materials can be found in table 13.

For this BSA, compared to the Hammond BSA, there was an increase in use of Aluminum. This was likely due to the higher energy of neutrons exiting the spallation target. These materials are able to scatter the neutrons more efficiently from higher energies, and absorb neutrons more readily. In addition, the BSA radius was on the wider end like the Hammond run. This was due to the head having a relatively larger area, and this additional scattering radius could contribute to some spectral weighting and shielding.

Best BSA Candidate for the Limited Material Case Study: Grant

The Grant run used the reduced list of materials see table 2 located in the Appendix, the cell culture medium model, the equation 3.2 fitness, and the PNS neutron source. Like the other cell culture medium model, this model was run with the intent of it being performed experimentally in a clinical proton center setting.

The optimum design given by the GNOWEE/MCNP Grant run had a fitness of 0.9914231. The optimum reaction occurred 0.9% of the time. For this BSA, the chosen source was the Lead target with a 100 Mev proton beam. When compared to the other PNS model, the lower proton energy fits an expectation of this model. Previously it was mentioned that lower neutron energies will increase the ideal reaction rate. As a result, it makes sense that the model optimized to the lower of the two origin energies. Like all previous BSA's, the Grant BSA length was 70 cm, and the internal BSA component structure remained the same. The BSA radii, and and materials can be found in the Appendix in tables 14 and 15. Also, the Grant BSA had a slimmer radius like the previous Malcolm model.

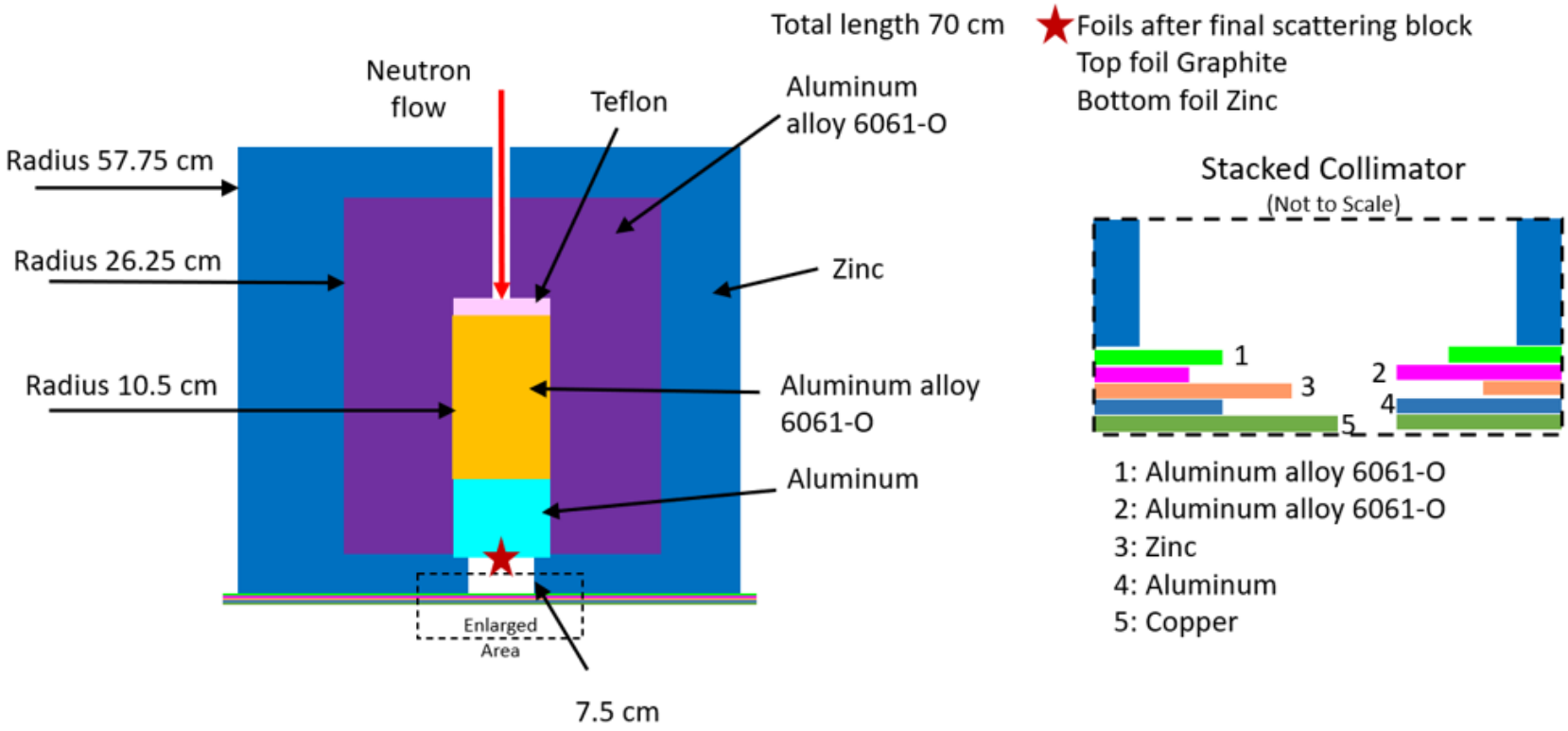

Figure 4.3: Visual depiction of Sattler BSA Design

This was again due to the decrease in target area, and lack of need for additional shielding for the cell culture medium target model. Figure 4.4 depicts the ideal BSA for the Grant run.

The optimum design had 9 collimators with the collimators opening centered on the center of the cell culture medium. This is expected as the neutrons should spread out to cover the cell culture medium surface. The leaf materials can be found in table 16. Again, the maximum number of collimators allowed for an increase in the thermal flux available. As this optimization only cared about reaction rate, and the volume of target to react was only 1 cell think, there is an increase in need for the highest amount of thermal neutron flux.

Similar to the Malcolm BSA, the Grant BSA mainly consisted of varieties of polyethylene. This was a result of the constraint of the reduced material library. The copious amounts of polyethylene was expected due to the properties of hydrogen to scatter and absorb neutrons.

Best BSA Candidate for the Tumor Location Change Case Study: Spielberg

The Spielberg run was different than any of the other runs. Like previously mentioned, this run used information from the previously completed Hammond run with an altered head set up. The materials and dimensions of the core BSA are identical to the optimum Hammond BSA, and those materials and dimensions can be found in tables 5 and 6 located in the Appendix. The difference that was observed in the BSA set up was the increase in leaf number, and changes in collimator material. While the BSA remained unchanged, the optimizer could still change the number and materials of the collimators. This decision was made to demonstrate the ability for the BSA to apply and potentially be used for other disease sites for BNCT. This would allow for the possibility of generalization for BNCT which could open the doors for future investigation to be performed in this realm. The change in the collimators can be seen in table 18 located in the Appendix. Figure 4.5 depicts the ideal BSA for the Malcolm run.

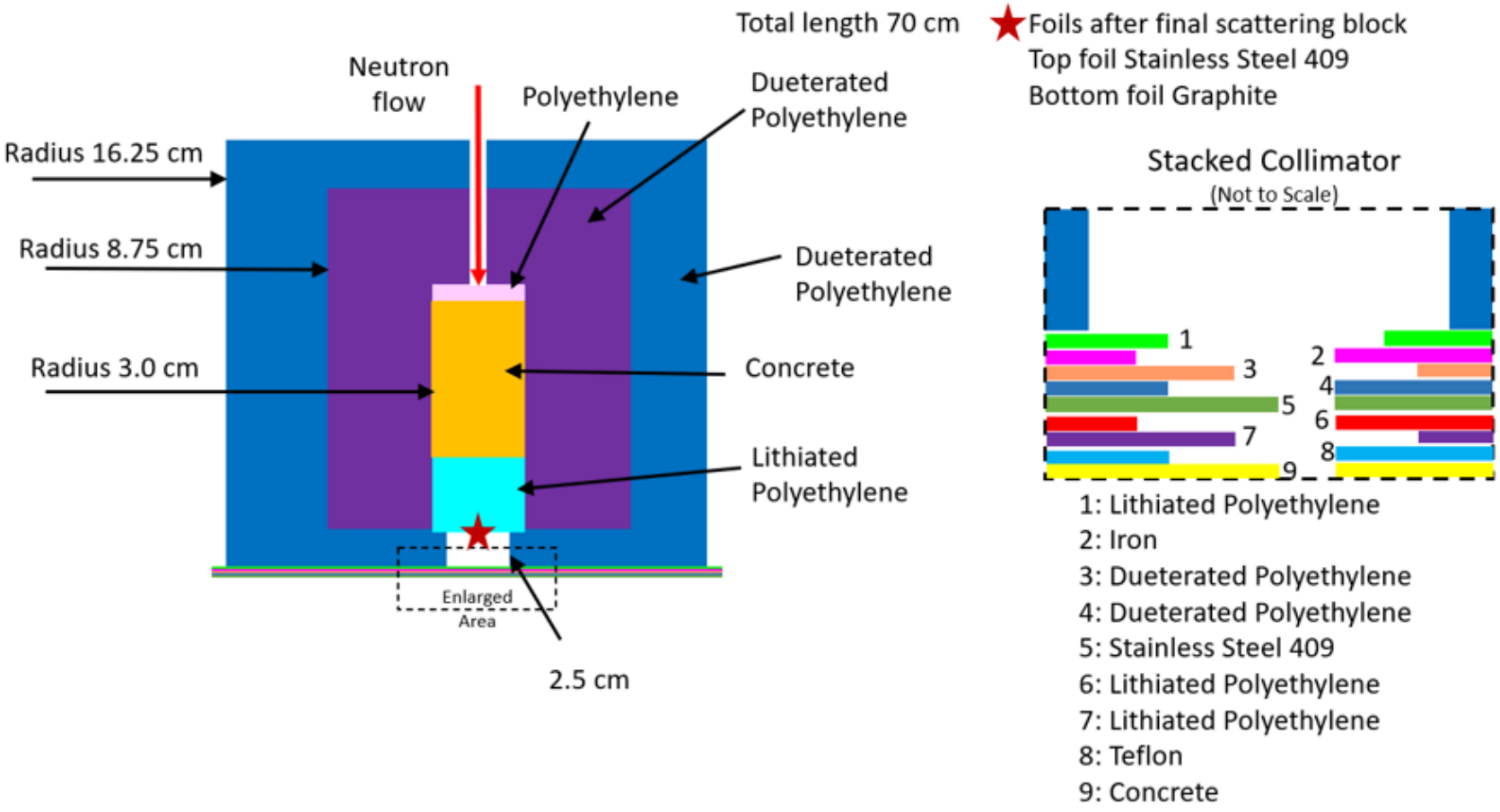

Figure 4.4: Visual depiction of Grant BSA Design

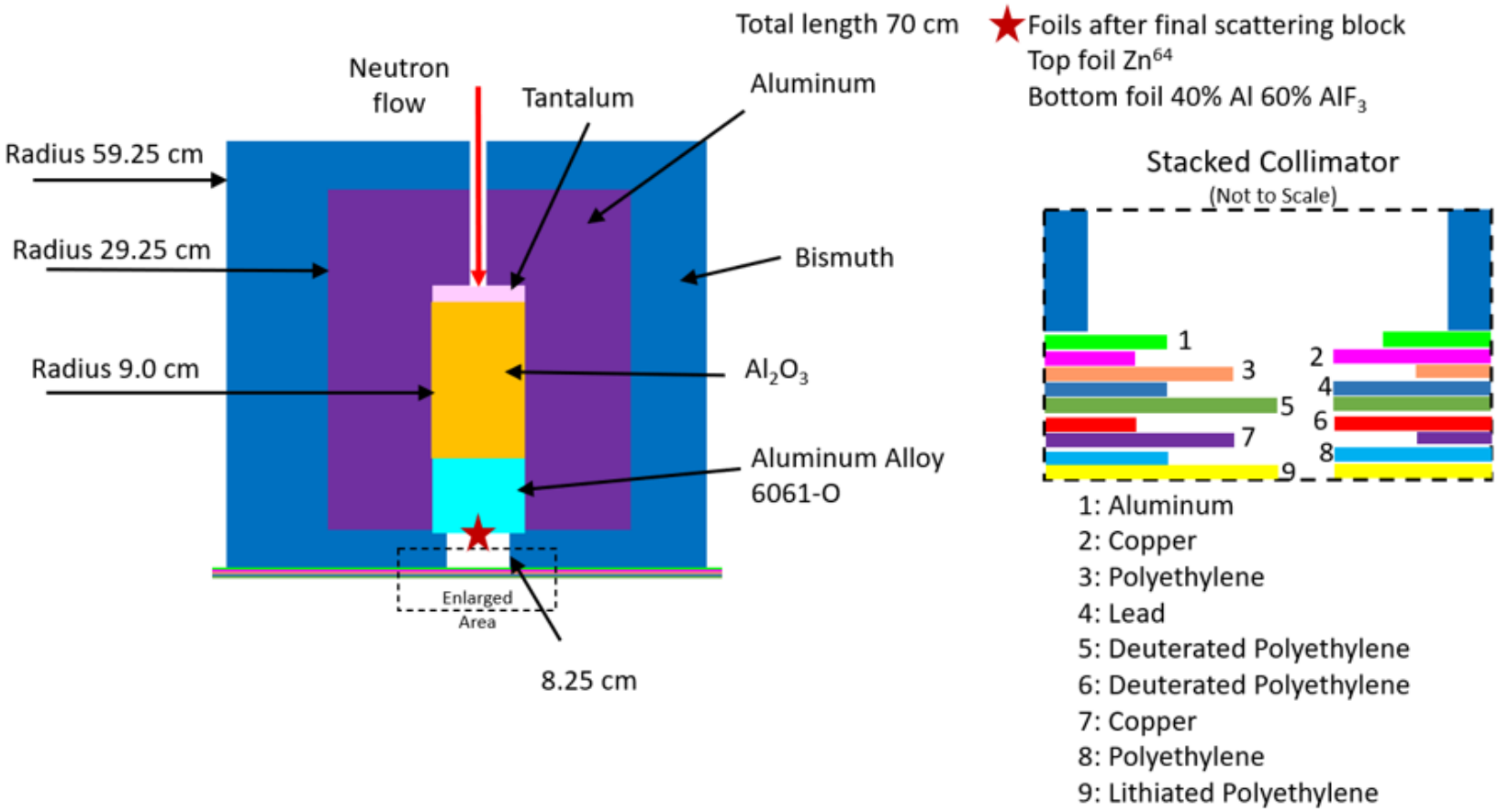

Figure 4.5: Visual depiction of Spielberg BSA Design

Compared to the materials Hammond run's collimators, there was an increase in polyethylene. Also, the optimizer chose the maximum number of collimators. These optimization decisions, allowed for an increase in thermal neutron flux, which was advantageous for this tumor site setup. Due to the tumor moving moving closer to the surface, there was the potential for an increased utilization for the thermal neutron flux instead of that same flux getting absorbed in the standard head setup. The increase in thermal flux utilization was demonstrated in the calculated doses from this model, shown in table 17. The increase in thermal flux and dose shows a potential future investigative avenue for BNCT. The increased use of thermal flux could provide inspiration for the use of BNCT for more surface level tumors which should be investigated in the future. In contrast, while the dose increased, there was a massive reduction in the amount of neutrons leaving the BSA. The calculated % of neutrons that survived the BSA was only 2.6%, but this was offset due to the increased reaction rate by the surviving thermal neutron flux. Like previous models, the calculated uncertainty also remained relatively low at 0.0026.

4.3 Comparison of the Neutron Flux Spectra for all the Case Studies

The following section depicts the neutron flux per unit lethargy spectra. Figures 4.6, 4.7, 4.8, 4.9, and 4.10 depict each of the simulated neutron spectra produced by each of the optimum BSA design. For each of these images, there is also a zoomed in view of the previously established optimum neutron flux for the standard head set up. This was left in a comparison for each of the models to show how differing inputs of the optimization will effect the optimization results. Each of the following spectra was modeled at the external surface of the head or cell culture medium model, featuring the surface area most likely to impact with the Boron doped target tissue.

While each of the initial neutron sources were different it is important to not that these spectra contain primarily thermal neutrons. This was more advantageous for the cell culture medium than the head model, as the neutrons have less material to pass through prior

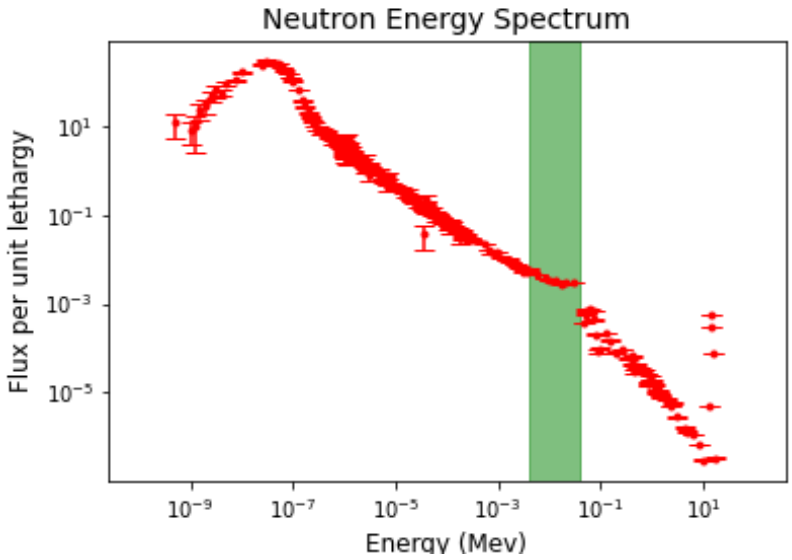

(a) Entirety of neutron spectrum produced by Hammond BSA

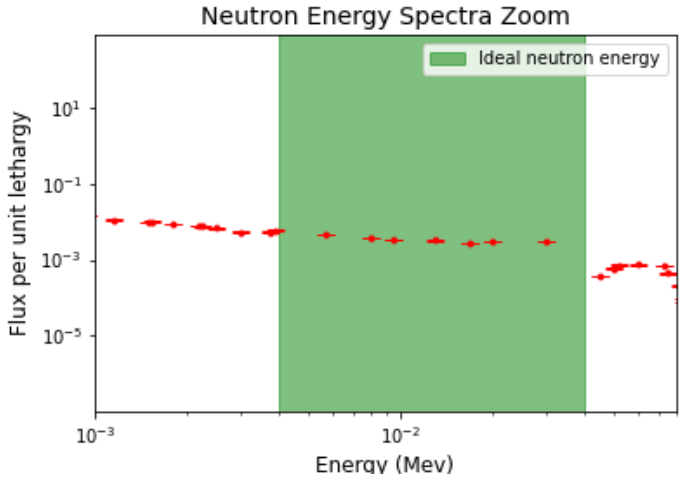

(b) Zoomed in view of neutron spectrum produced by Hammond BSA

Figure 4.6: Hammond BSA produced neutron spectrum

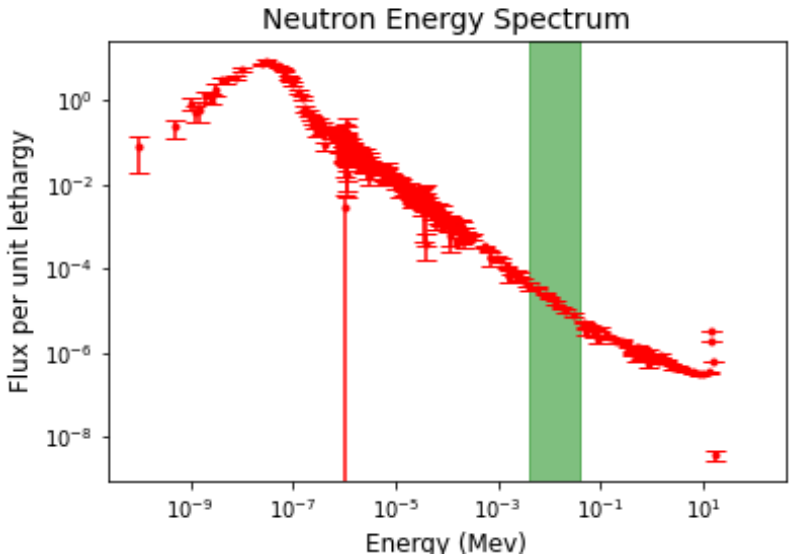

(a) Entirety of neutron spectrum produced by Malcolm BSA

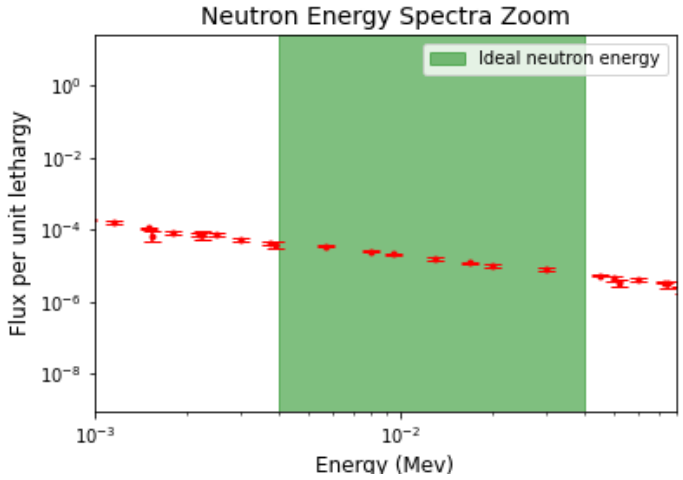

(b) Zoomed in view of neutron spectrum produced by Malcolm BSA

Figure 4.7: Malcolm BSA produced neutron spectrum

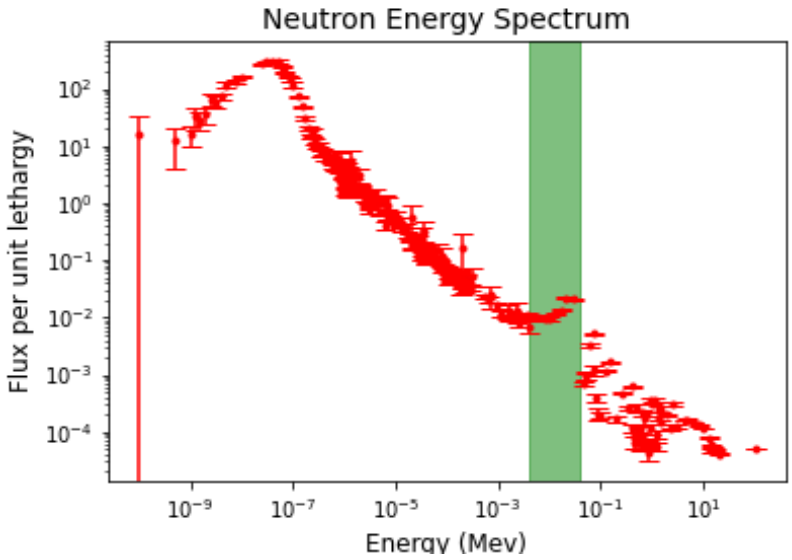

(a) Entirety of neutron spectrum produced by Sattler BSA

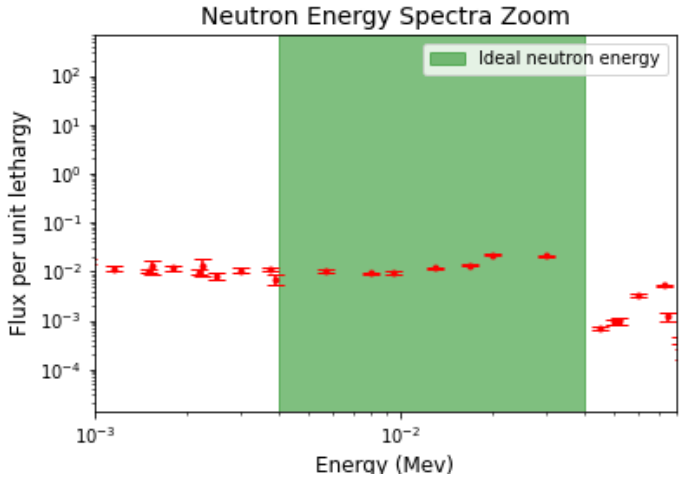

(b) Zoomed in view of neutron spectrum produced by Sattler BSA

Figure 4.8: Sattler BSA produced neutron spectrum

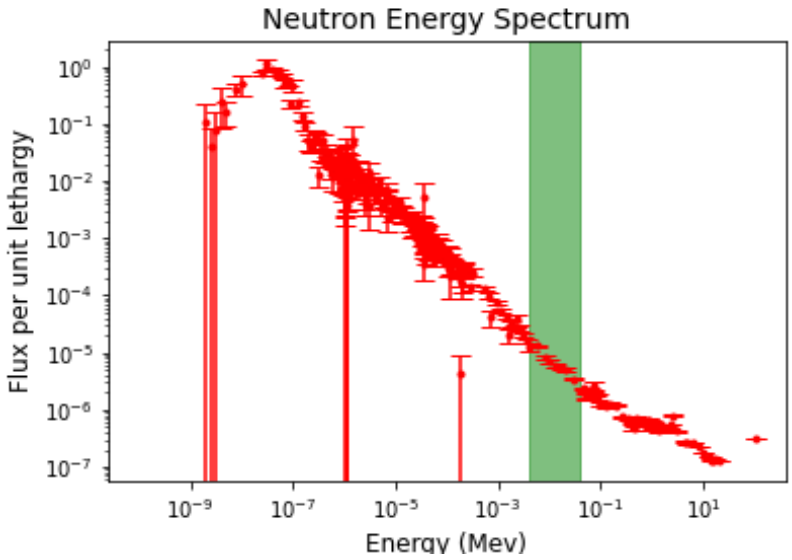

(a) Entirety of neutron spectrum produced by Grant BSA

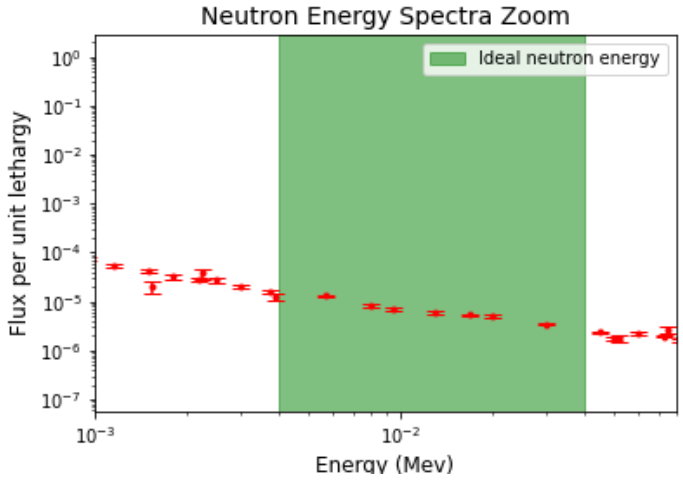

(b) Zoomed in view of neutron spectrum produced by Grant BSA

Figure 4.9: Grant BSA produced neutron spectrum

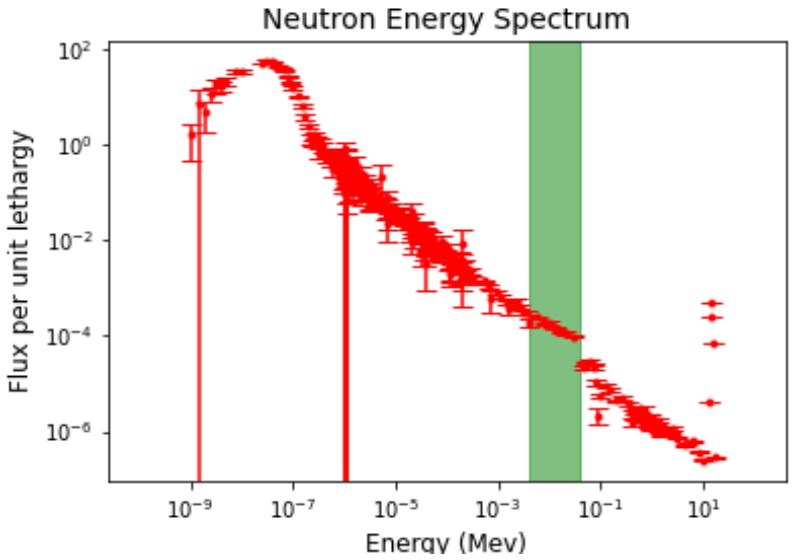

(a) Entirety of neutron spectrum produced by Spielberg BSA

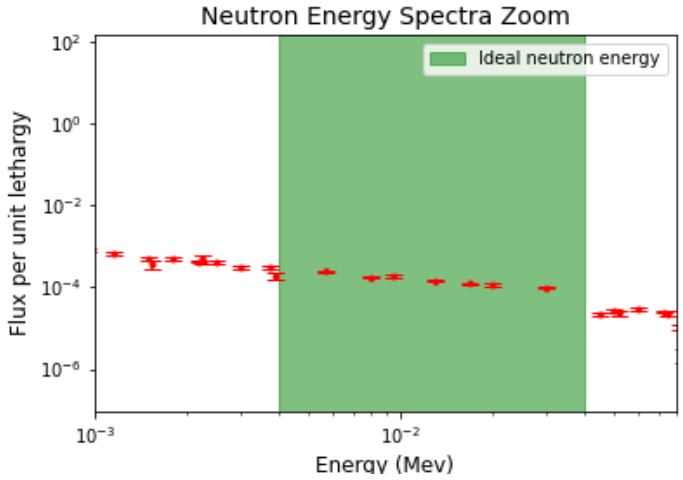

(b) Zoomed in view of neutron spectrum produced by Spielberg BSA

Figure 4.10: Grant BSA produced neutron spectrum

to interacting with the target site. The cell culture medium model optimized the optimal reaction rate, and the cross section increases inversely with the neutron energy. When comparing the head models, there is some observable peak around the 30 Kev neutron energy. This was expected, as one of the figures of merit GNOWEE/MCNP considered, was the optimum energy range of 4-40 Kev.

4.4 Population Fitness Analysis

One of the more interesting pieces of GNOWEEE/MCNP is the progression of the parent fitnessses throughout the optimization run. Figure 4.11 contains the scatter plot for each of the parent fitness groups. While each run didn't have the same amount of generations, it was likely that a local optimum was reached for each run. Every plot followed the same exponential shape that is expected for an optimization process, and while there was varying time to reach a plateau, for each run it could be argued that a plateau was reached, and the optimization ended due to the identical parent lists.

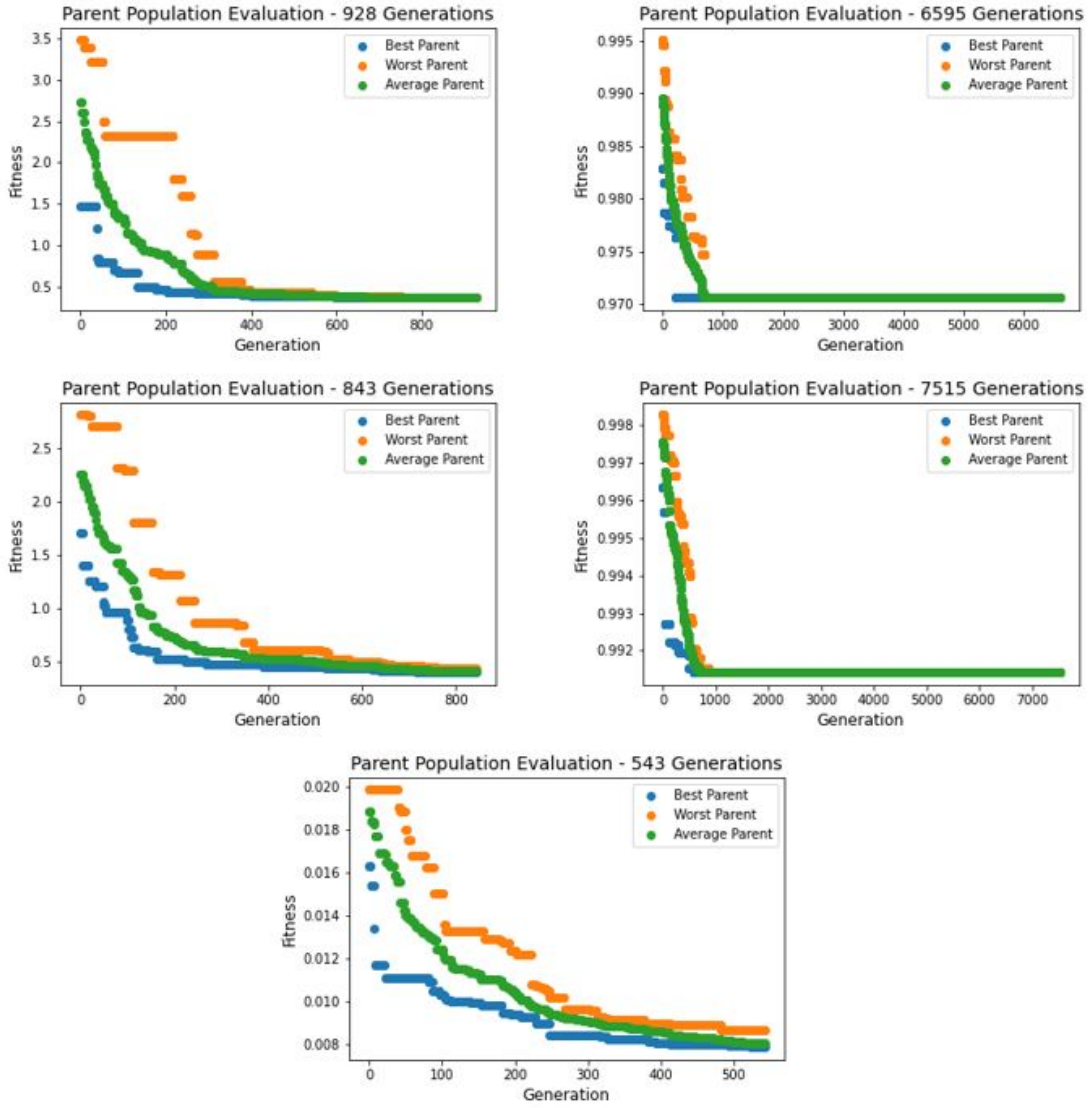

Figure 4.11: Fitness progression throughout each GNOWEE/MCNP run

Chapter 5

Conclusions

This thesis introduces and aims to demonstrate the advantages of using high level optimization, i.e. metaheurustic optimization methods, coupled with monte carlo radiation transport codes, i.e. MCNP6.2, for efficient designing of BSAs for Boron NEutron Capture Therapy (NCT) treatments. In numerous research fields there is an interest in accurate and efficient methodologies that can be used to tailor available neutron spectra to the specific application needs, thus the work focus meets the needs of a wider field of interest.

The main goal of this dissertation is the development of an efficient optimization tool for tailoring neutron spectra produced in various neutron generating facilities for BNCT application. The dissertation research included specific steps: identification of the optimization software, i.e GNOWEE, the transport simulations code, MCNP6.2; development of a framework that couple the optimization code with MCNP6.2; the identification of the figure of merit (FOM) for optimizing the BSA design for BNCT.

Previous BNCT research has shown particular difficulties in designing and assembling materials to customize the neutron spectra using neutron filters or neutron thermalization using low-Z moderators. A primary limitation in the past BSA design procedures was a very slow and time-consuming parametric study approach. Thus, there was a need for a more coherent, generalized, and efficient optimization methodology, that would allow for an automated approach to optimal choice of materials and geometric. The UC Berkeley developed software Gnowee, here coupled with MCNP6.2 solved this problem. The BSA design process resembles a complex multidimensional and multi-variable optimization

problem, and currently similar optimization methodology applicable to neutron energy tailoring does not exist.

To demonstrate the flexibility of the developed modeling framework for BNCT, this study introduced five case scenarios for five different setups. The setups included a head test case with two tumors' depths and a cell culture, to mimic a possible validation experiment scenario, and different starting neutron sources. The dimensions of the head model area as follows: total head 9.5 cm, skin thickness 0.148cm, skull thickness 0.85cm, healthy tissue radius 8.702cm, and a tumor radius of 1cm located at the center of the head. For the second test case, the tumor was moved from the center point to 5cm closer to the surface. The cell culture medium setup had the dimensions as follows: 6.75x6.75 cm^2, thickness of 1 cell, and 0.2cm of blood on top of the cell layer. One set of optimizations could chose from a group of neutron sources: Deuterium-Deuterium (D-D), Deuterium-Tritium (D-T), and a fast neutron source (FNS). The other set of optimizations could chose from 100 or 200 Mev protons incident on either a Pb or W target. Most previous BSA optimizations only optimized one BSA per source and tumor, in this work, the secondary setup demonstrated a previous unexplored possibility for generalization of BSA's for BNCT. The stacked collimator optimization provided the possibility for a center to treat different tumor sites with a singular BSA.

When evaluating the cases using a head tumor set up, a clear advantage was identified to using neutron source design over the available proton neutron spallation set up. This can be contributed to the increase in dose at all sites most notable the tumor. Specifically, there was an 555,555× increase in calculated dose between the Hammond and Sattler models. When considering the cell culture medium setups, both used comparable materials with the neutron source having 3% of the optimal alpha reaction compared to the proton neutron spallation having an optimal reaction rate of 0.9%. That being said, the abundance of proton centers in the US leaves open the possibility that there could be further exploration for the possibility of proton spallation based BNCT. Comparing the 4 independent BSA's the most observable discrepancy was with the number of collimator increase between the head and cell culture medium models (5 vs 9). The difference in collimator number can be linked directly to the resultant neutron spectrum. As the objectives for the optimizations were

different, the increase in collimator number led to an increase in thermal neutron flux and therefore an increase in reaction rate. Another objective of this project was to demonstrate the potential for one BSA to treat multiple tumor sites. To do so the Hammond BSA, with the potential for further collimator optimization, was optimized to a head with a tumor site closer to the surface. This optimum produced a model with 9 collimators that allowed for increased thermal flux. At the same time, the tumor location closer to the surface allowed for a higher utilization of the thermal flux leading to an increased ratio of equivalent doses between the tumor and surrounding tissue and skin. The improved figures of merit allows for the conclusions that one BSA could be used to treat multiple tumor sites, with the use of the stacked collimator, and that tumor sites that use more of the thermal flux are more advantageous for BNCT usage than ones that do not take advantage of the thermal neutron flux.The development of a generalized and validated optimization framework will expand the capabilities of BNCT in existing facilities for various tumors at a fraction of the cost in terms of manpower and research effort rather than building and designing alternative facilities. The capabilities developed in this research are unique on many levels. This research leveraged and expanded upon the previous concept of BSA and ETAs using high level optimization techniques and simple experimental setups at existing facilities and cheap neutron sources and of previous collimator designs.

Chapter 6

Future work

This presented research work's goal was to enhance the BNCT opportunities as a cancer treatment by looking to solve the lack of ideal neutron source. Advanced optimization algorithms, such as metaheurisitcs here used, can support and expand further investigation into BNCT. Nevertheless, more work is required to validate the optimization code used for designing the BSA, to speed up the optimization methodology, to demonstrate its expanded application to different tumors, etc. The authors below lays down few future directions for this work.

6.1 Future Optimization

There is still work that could be done as the optimization code is made available and open to the nuclear medical community for BNCT and other medical applications. The current GNOWEE/MCNP for BNCT package allows to design efficient BSA for various neutron generator environments, which was the objective of this work. However, many features could be further expanded:

- Investigation of each figure of merit independently through multi-objective GNOWEE/MCNP run. (i.e. solo dose, solo cost, or solo desired spectra objectives)

- Investigation for each collimator to be symmetric in the X and Y planes. The previous modeling allowed for asymmetric collimators, further investigation into how symmetric collimator fields could prove beneficial.

- Investigation of an entire patient for more complete and accurate dosimetry. For these models, only a small model of a human head was considered, future modeling and experimentation could use more complete phantoms for more accurate dosimetry.

- Machine learning techniques could be employed in order to improve in the areas of "learning speed", non-linear data handling, and complex feature identification.

6.2 Possible BNCT Experiment

Finally, this work opens the door for a potential BNCT validation experiments. In order to validate the abilities to design flexible BSA for various neutron sources, experiments need to be performed. Also, Calibration and experimental uncertainties can affect the optimization results besides the data uncertainties; seeing those details in the final results would be useful while performing the optimization. One of the first experiment proposed is to use tumor cell lines grown and doped with Boron, that are irradiated by a DD/DT and PNS source and a BSA in combination with detectors. This first experiment will provide initial data to understand cell death rate by neutron interaction with Boron and provide an idea of the neutron flux exiting the BSA, and of any secondary particle produced by the BSA. More complicated experiments could follow using tumors inside animals, i.e. rats, to validate the optimization methodology for various tumor size and depths and validate the ratio of tumor dose over healthy tissue, to insure the selective nature of the treatment.

Bibliography

[1] AttCHAMBEAU, J. (1970). The effect of increasing exposures of the'˜ reaction on the skin of man'. *Radiology*, 94:179–187. 6

[2] Bevins, J. E. (2017). *Targeted modification of neutron energy spectra for national security applications*. University of California, Berkeley. 3, 21

[3] Bevins, J. E. and Slaybaugh, R. N. (2019). Gnowee: a hybrid metaheuristic optimization algorithm for constrained, black box, combinatorial mixed-integer design. *Nuclear Technology*, 205(4):542–562. 3, 11

[4] Busch, C. and Delpillis, A. (2023). Gnowee_mulitnsga. https://github.com/NE-UTK-Computation-Lab/Gnowee_Mulit-NSGA. 14

[5] Buschmann, M., Majercakova, K., Sturdza, A., Smet, S., Najjari, D., Daniel, M., Pötter, R., Georg, D., and Seppenwoolde, Y. (2018). Image guided adaptive external beam radiation therapy for cervix cancer: evaluation of a clinically implemented plan-of-the-day technique. *Zeitschrift für Medizinische Physik*, 28(3):184–195. 1

[6] Cao, D., Afghan, M. K., Ye, J., Chen, F., and Shepard, D. M. (2009). A generalized inverse planning tool for volumetric-modulated arc therapy. *Physics in Medicine & Biology*, 54(21):6725. 11

[7] Čufar, A., Batistoni, P., Ghani, Z., Giacomelli, L., Lengar, I., Loreti, S., Milocco, A., Popovichev, S., Pillon, M., Rigamonti, D., et al. (2018). Modelling of the neutron production in a mixed beam dt neutron generator. *Fusion engineering and design*, 136:1089–1093. 7

[8] Das, B. K., Shyam, A., Das, R., and Rao, A. (2013). Development of compact dd neutron generator. *Instruments and Experimental Techniques*, 56(2):130–133. 7

[9] Du, W., Cho, S. H., Zhang, X., Hoffman, K. E., and Kudchadker, R. J. (2014). Quantification of beam complexity in intensity-modulated radiation therapy treatment plans. *Medical physics*, 41(2):021716. 11

[10] Fantidis, J., Saitioti, E., Bandekas, D., and Vordos, N. (2013). Optimised bnct facility based on a compact dd neutron generator. *International Journal of Radiation Research*, 11(4):207. 7

[11] Goitein, M. and Jermann, M. (2003). The relative costs of proton and x-ray radiation therapy. *Clinical Oncology*, 15(1):S37–S50. 2

[12] Hatanaka, H., Sweet, W., Sano, K., and Ellis, F. (1991). The present status of boron-neutron capture therapy for tumors. *Pure and applied chemistry*, 63(3):373–374. 7

[13] Heimberger, A. B., Crotty, L. E., Archer, G. E., McLendon, R. E., Friedman, A., Dranoff, G., Bigner, D. D., and Sampson, J. H. (2000). Bone marrow-derived dendritic cells pulsed with tumor homogenate induce immunity against syngeneic intracerebral glioma. *Journal of neuroimmunology*, 103(1):16–25. 2, 10

[14] Holland, E. C. (2000). Glioblastoma multiforme: the terminator. *Proceedings of the National Academy of Sciences*, 97(12):6242–6244. 3, 10

[15] Karaoglu, A., Arce, P., Obradors, D., Lagares, J. I., and Unak, P. (2018). Calculation by gamos/geant4 simulation of cellular energy distributions from alpha and lithium-7 particles created by bnct. *Applied Radiation and Isotopes*, 132:206–211. 2

[16] Le, F., WH, S., HB, L., and JS, R. (1954). Neutron capture therapy of gliomas using boron. *Transactions of the American Neurological Association*, 13(79th Meeting):110–113. 6

[17] Locher, G. (1936). Ab-x nct. *Am. J. Roentgenol*, 36:1–13. 6

[18] Mihailidis, D. (2019). The physics & technology of radiation therapy. 2nd edition. pn mcdermott & cg orton, authors. madison, wi: Medical physics publishing, 2018. 870. pp. price: $165.00. isbn: 9781930524989. *Medical Physics*, 46(8):3751–3752. 1, 2, 8, 10

[19] Mishima, Y., Ichihashi, M., Hatta, S., Honda, C., Yamamura, K., Nakagawa, T., Obara, H., Shirakawa, J., Hiratsuka, J., and Taniyama, K. (1989). First human clinical trial of melanoma neutron capture. diagnosis and therapy. *Strahlentherapie und Onkologie: Organ der Deutschen Rontgengesellschaft...[et al]*, 165(2-3):251–254. 7

[20] Moss, R. L. (2014). Critical review, with an optimistic outlook, on boron neutron capture therapy (bnct). *Applied Radiation and Isotopes*, 88:2–11. 6

[21] Nobakht, E. and Fouladi, N. (2019). Feasibility study on the use of 230mev proton cyclotron in proton therapy centers as a spallation neutron source for bnct. *Reports of Practical Oncology and Radiotherapy*, 24(6):644–653. 2, 8

[22] Oldham, M., Neal, A., and Webb, S. (1995). A comparison of conventional 'forward planning'with inverse planning for 3d conformal radiotherapy of the prostate. *Radiotherapy and Oncology*, 35(3):248–262. 11

[23] Pevey, J. L., Salyer, C., Chvala, O., Sobes, V., and Hines, J. W. (2021). Multi-objective design optimization of a fast spectrum nuclear experiment facility using artificial intelligence. *Annals of Nuclear Energy*, 162:108476. 7, 8

[24] Riley, J. C. (2005). Estimates of regional and global life expectancy, 1800–2001. *Population and development review*, 31(3):537–543. 1

[25] Salyer, C. I. (2022). Meta-heuristic optimization techniques for the production of medical isotopes through special target design. 8

[26] Schubert, L. K., Gondi, V., Sengbusch, E., Westerly, D. C., Soisson, E. T., Paliwal, B. R., Mackie, T. R., Mehta, M. P., Patel, R. R., Tomé, W. A., et al. (2011). Dosimetric comparison of left-sided whole breast irradiation with 3dcrt, forward-planned imrt, inverse-planned imrt, helical tomotherapy, and topotherapy. *Radiotherapy and Oncology*, 100(2):241–246. 11

[27] Slatkin, D. N. (1991). A history of boron neutron capture therapy of brain tumours: postulation of a brain radiation dose tolerance limit. *Brain*, 114(4):1609–1629. 6

[28] Verbeke, J. M. (2000). Development of high-intensity dd and dt neutron sources and neutron filters for medical and industrial applications. x, 3, 4, 8, 9, 19

[29] Wang, L., Wang, S., Chu, P., Ho, C., Jiang, S., Liu, Y. H., Liu, Y., Liu, H., Peir, J., Chou, F., et al. (2011). Bnct for locally recurrent head and neck cancer: preliminary clinical experience from a phase i/ii trial at tsing hua open-pool reactor. *Applied Radiation and Isotopes*, 69(12):1803–1806. 7

[30] Werner, C. J., Bull, J. S., Solomon, C. J., Brown, F. B., McKinney, G. W., Rising, M. E., Dixon, D. A., Martz, R. L., Hughes, H. G., Cox, L. J., Zukaitis, A. J., Armstrong, J. C., Forster, R. A., and Casswell, L. (2018). Mcnp version 6.2 release notes. 3, 8, 12, 13

[31] Yagata, H., Kajiura, Y., and Yamauchi, H. (2011). Current strategy for triple-negative breast cancer: appropriate combination of surgery, radiation, and chemotherapy. *Breast Cancer*, 18:165–173. 1

[1]

Appendix

Material Lists

Below are tables containing the expansive and reduced material lists used in the GNOWEE/MCNP runs.

Table 1: Expansive material list

6Li	Al	Pb
Fe	Bi	Cu
Zr	Ni	In
Ta	Au	Cu63
Zn	Zn64	Ti
Ti46	Ir	Graphite
6LiF	63.6 a/o H3 + 36.4 a/o Ti	Al2O3
40% Al 60% AlF3	Lithiated polyethylene	Aluminum alloy 6061-O
Stainless Steel 409	Deuterated Polyethylene	Concrete
Polyethylene	Teflon	BeO

Table 2: Reduced material list

Pb	Fe
Graphite	Lithiated polyethylene
Concrete	Polyethylene
Teflon	Stainless Steel 409
Al	Dueterated Polyethylene

Results Tables

Below is the table that details the number of evaluations and the total evaluation time for each model.

Below is the table for comparative doses for Hammond and Sattler models.

Table 3: Evaluation time for each BSA model

GNOWEE/MCNP Run	Number of Evaluations	Total time	Effective Time
Hammond	4,521	132.75 Hours	1.75 min
Malcolm	11,160	262.5 Hours	1.41 min
Sattler	4,062	113 Hours	1.67 min
Grant	12,612	179.3 Hours	0.85 min

Table 4: Calculated Doses from Hammond and Sattler models

Area of Dose	Hammond	Sattler
Tumor	20.03 Sv	3.62*E-5 Sv
Tissue	2.62 Sv	3.57*E-6 Sv
Skin	1.43 Sv	1.29E-6 Sv

Run Tables

Below are tables containing tables for the 4 optimum GNOWEE/MCNP runs. Each run has tables below contain information about the optimum dimensions, materials, and leaf materials.

Table 5: Hammond BSA measurements

Object Measured	Measurement
BSA length	70 cm
External Radius	59.25 cm
Reflector radius	29.25 cm
Internal Scattering Block Radius	9.0 cm

Table 6: Hammond BSA materials

BSA Component	Component Material
Outer shield	Bismuth
Reflector	Aluminum
Top Scattering Block	Tantalum
Middle Scattering Block	Al2O3
Bottom Scattering Block	Aluminum Alloy 6061-O
Top Foil	Zn64
Bottom Foil	40% Al 60% AlF3

Table 7: Hammond Leaf materials

Leaf#	Leaf Material
Leaf 1 (top leaf)	Copper
Leaf 2	Copper
Leaf 3	Concrete
Leaf 4	Aluminum
Leaf 5 (bottom leaf)	Zirconium

Table 8: Malcolm BSA measurements

Object Measured	Measurement
BSA length	70 cm
External Radius	16.25 cm
Reflector radius	8.75 cm
Internal Scattering Block Radius	3.0 cm

Table 9: Malcolm BSA materials

BSA Component	Component Material
Outer shield	Polyethylene
Reflector	Polyethylene
Top Scattering Block	Polyethylene
Middle Scattering Block	Iron
Bottom Scattering Block	Polyethylene
Top Foil	Lead
Bottom Foil	Lithiated Polyethylene

Table 10: Malcolm Leaf materials

Leaf #	Leaf material
Leaf 1 (top leaf)	Concrete
Leaf 2	Iron
Leaf 3	Iron
Leaf 4	Polyethylene
Leaf 5	Deuterated Polyethylene
Leaf 6	Polyethylene
Leaf 7	Lithiated Polyethylene
Leaf 8	Lithiated Polyethylene
Leaf 9 (bottom leaf)	Concrete

Table 11: Sattler BSA measurements

Object Measured	Measurement
BSA length	70 cm
External Radius	57.75 cm
Reflector radius	26.25 cm
Internal Scattering Block Radius	10.5 cm

Table 12: Sattler BSA materials

BSA Component	Component Material
Outer shield	Zinc
Reflector	Aluminum alloy 6061-O
Top Scattering Block	Teflon
Middle Scattering Block	Aluminum alloy 6061-O
Bottom Scattering Block	Aluminum
Top Foil	Graphite
Bottom Foil	Zinc

Table 13: Sattler Leaf materials

Leaf #	Leaf material
Leaf 1 (top leaf)	Aluminum alloy 6061-O
Leaf 2	Aluminum alloy 6061-O
Leaf 3	Zinc
Leaf 4	Aluminum
Leaf 5 (bottom leaf)	Copper

Table 14: Grant BSA measurements

Object Measured	Measurement
BSA length	70 cm
External Radius	16.25 cm
Reflector radius	8.75 cm
Internal Scattering Block Radius	3.0 cm

Table 15: Grant BSA materials

BSA Component	Component Material
Outer shield	Deuterated Polyethylene
Reflector	Deuterated Polyethylene
Top Scattering Block	Polyethylene
Middle Scattering Block	Concrete
Bottom Scattering Block	Lithiated Polyethylene
Top Foil	Stainless Steel 409
Bottom Foil	Graphite

Table 16: Grant Leaf materials

Leaf #	Leaf material
Leaf 1 (top leaf)	Lithiated Polyethylene
Leaf 2	Iron
Leaf 3	Deuterated Polyethylene
Leaf 4	Deuterated Polyethylene
Leaf 5	Stainless Steel 409
Leaf 6	Lithiated Polyethylene
Leaf 7	Lithiated Polyethylene
Leaf 8	Teflon
Leaf 9 (bottom leaf)	Concrete

Table 17: Calculated Doses from the Spielberg model

Area of Dose	Spielberg
Tumor	31.33 Sv
Tissue	0.77 Sv
Skin	0.17 Sv

Table 18: Spielberg Leaf materials

Leaf #	Leaf material
Leaf 1 (top leaf)	Aluminum
Leaf 2	Copper
Leaf 3	Polyethylene
Leaf 4	Lead
Leaf 5	Deuterated Polyethylene
Leaf 6	Deuterated Polyethylene
Leaf 7	Copper
Leaf 8	Polyethylene
Leaf 9 (bottom leaf)	Lithiated Polyethylene

Vita

Christopher Busch is from Spartanburg, South Carolina and attended Dorman High school. Christopher participated in marching band and golf growing up and his interest in collegiate marching band is what drove him to first consider attending the University of Tennessee. After considering future career paths, nuclear engineering piqued his interest and upon his acceptance to the Tickle college of engineering, he began his undergraduate degree in the Fall of 2017. Christopher worked in radio-pharmaceutical development, and detector manufacturing during his time as an undergraduate. Immediately post graduation, he began working towards a Master's Degree in Medical Physics. Post graduate studies, Christopher will begin a residency in therapeutic medical physics with the goal to become a top clinical physicist. He hopes to bring his expertise and knowledge to further impact and improve patient care throughout the medical physics industry.